NASA/TM-2009-214651

Stability and Control Analysis of the F-15B Quiet Spike™ Aircraft

Shaun C. McWherter and Cheng M. Moua
NASA Dryden Flight Research Center
Edwards, California

Joseph Gera
AS&M, Inc.
Edwards, California

Timothy H. Cox
NASA Dryden Flight Research Center
Edwards, California

August 2009

NASA STI Program ... in Profile

Since its founding, NASA has been dedicated to the advancement of aeronautics and space science. The NASA scientific and technical information (STI) program plays a key part in helping NASA maintain this important role.

The NASA STI program operates under the auspices of the Agency Chief Information Officer. It collects, organizes, provides for archiving, and disseminates NASA's STI. The NASA STI program provides access to the NASA Aeronautics and Space Database and its public interface, the NASA Technical Report Server, thus providing one of the largest collections of aeronautical and space science STI in the world. Results are published in both non-NASA channels and by NASA in the NASA STI Report Series, which includes the following report types:

- TECHNICAL PUBLICATION. Reports of completed research or a major significant phase of research that present the results of NASA Programs and include extensive data or theoretical analysis. Includes compilations of significant scientific and technical data and information deemed to be of continuing reference value. NASA counterpart of peer-reviewed formal professional papers but has less stringent limitations on manuscript length and extent of graphic presentations.

- TECHNICAL MEMORANDUM. Scientific and technical findings that are preliminary or of specialized interest, e.g., quick release reports, working papers, and bibliographies that contain minimal annotation. Does not contain extensive analysis.

- CONTRACTOR REPORT. Scientific and technical findings by NASA-sponsored contractors and grantees.

- CONFERENCE PUBLICATION. Collected papers from scientific and technical conferences, symposia, seminars, or other meetings sponsored or co-sponsored by NASA.

- SPECIAL PUBLICATION. Scientific, technical, or historical information from NASA programs, projects, and missions, often concerned with subjects having substantial public interest.

- TECHNICAL TRANSLATION. English-language translations of foreign scientific and technical material pertinent to NASA's mission.

Specialized services also include creating custom thesauri, building customized databases, and organizing and publishing research results.

For more information about the NASA STI program, see the following:

- Access the NASA STI program home page at *http://www.sti.nasa.gov*

- E-mail your question via the Internet to help@sti.nasa.gov

- Fax your question to the NASA STI Help Desk at 443-757-5803

- Phone the NASA STI Help Desk at 443-757-5802

- Write to:
  NASA STI Help Desk
  NASA Center for AeroSpace Information
  7115 Standard Drive
  Hanover, MD 21076-1320

NASA/TM-2009-214651

Stability and Control Analysis of the F-15B Quiet Spike™ Aircraft

Shaun C. McWherter and Cheng M. Moua
NASA Dryden Flight Research Center
Edwards, California

Joseph Gera
AS&M, Inc.
Edwards, California

Timothy H. Cox
NASA Dryden Flight Research Center
Edwards, California

National Aeronautics and
Space Administration

Dryden Flight Research Center
Edwards, California 93523-0273

August 2009

NOTICE

Use of trade names or names of manufacturers in this document does not constitute an official endorsement of such products or manufacturers, either expressed or implied, by the National Aeronautics and Space Administration.

Available from:

NASA Center for AeroSpace Information
7115 Standard Drive
Hanover, MD 21076-1320
(443) 757-5802

ABSTRACT

The primary purpose of the Quiet Spike™ flight research program was to analyze the aerodynamic, structural, and mechanical proof-of-concept of a large multi-stage telescoping nose spike installed on the National Aeronautics and Space Administration Dryden Flight Research Center (Edwards, California) F-15B airplane. This report describes the preflight stability and control analysis performed to assess the effect of the spike on the stability, controllability, and handling qualities of the airplane; and to develop an envelope expansion approach to maintain safety of flight. The overall flight test objective was to collect flight data to validate the spike structural dynamics and loads model up to Mach 1.8. Other objectives included validating the mechanical feasibility of a morphing fuselage at operational conditions and determining the near-field shock wave characterization. The two main issues relevant to the stability and control objectives were the effects of the spike-influenced aerodynamics on the F-15B airplane flight dynamics, and the air data and angle-of-attack sensors. The analysis covered the sensitivity of the stability margins, and the handling qualities due to aerodynamic variation and the maneuvering limitations of the F-15B Quiet Spike™ configuration. The results of the analysis and the implications for the flight test program are also presented.

NOMENCLATURE

ARI	aileron to rudder interconnect
BAS	bare airframe stability
BL	baseline airplane model
CAP	control anticipation parameter, g^{-1} s^{-2}
CAS	control augmentation system
$CD_{\alpha\beta}$	drag increase due to angle-of-attack and sideslip variations, deg^{-1}
CFD	computational fluid dynamics
$C_{l_{da}}$	rolling moment due to aileron deflection, deg^{-1}
$C_{l_{da}}$_table	baseline airplane look up for rolling moment due to aileron deflection, deg^{-1}
$C_{l_{dr}}$	rolling moment due to rudder deflection, deg^{-1}
$C_{l_{dt}}$	rolling moment due to differential stabilator deflection, deg^{-1}
C_{l_p}	rolling moment due to roll rate variation, rad^{-1}
C_{l_r}	rolling moment due to yaw rate variation, rad^{-1}
C_{l_β}	rolling moment due to sideslip variation, deg^{-1}
$C_{L_{SPK}}$	Lift contribution of the spike
C_{L_α}	lift curve slope, deg^{-1}
$C_{m_{dh}}$	pitching moment due to symmetric stabilator deflection, deg^{-1}
C_{m_q}	pitching moment due to pitch rate variation, rad^{-1}
$C_{m_{SPK}}$	total non-dimensional pitching moment contribution of the spike

C_{m_0}	non-dimensional zero lift pitching moment coefficient
C_{m_α}	pitching moment due to angle-of-attack variation, deg^{-1}
$C_{n_{da}}$	yawing moment due to aileron deflection, deg^{-1}
$C_{n_{dr}}$	yawing moment due to rudder deflection, deg^{-1}
$C_{n_{dt}}$	yawing moment due to differential stabilator deflection, deg^{-1}
C_{n_p}	yawing moment due to roll rate variation, rad^{-1}
C_{n_r}	yawing moment due to yaw rate variation, rad^{-1}
$C_{n_{SPK}}$	total non-dimensional yawing moment contribution of the spike
$C_{n_{SPK}}$ _offset	non-dimensional uncertainty bias on spike yawing moment
$C_{n_{SPK}}$ _table	nominal non-dimensional yawing moment contribution of the spike
C_{n_β}	yawing moment due to sideslip variation, deg^{-1}
$C_{y_{da}}$	side force due to aileron surface deflection, deg^{-1}
$C_{y_{dr}}$	side force due to rudder surface deflection, deg^{-1}
$C_{y_{dt}}$	side force due to the differential tail deflection, deg^{-1}
$C_{y_{SPK}}$	non-dimensional side force contribution of spike
C_{y_β}	side force due to sideslip, deg^{-1}
deg	degrees
Da	aileron deflection, deg
DAI	Desktop Aeronautics Incorporated
Dep	pitch stick deflection, in
DFRC	Dryden Flight Research Center
Dh	symmetric stabilator position, deg
DOF	degree-of-freedom
DR	symmetric rudder position, deg
Dt	differential stabilator deflection, deg
DTA	Desktop Aeronautics Incorporated implemented spike model
fps	feet per second
FS	fuselage station, in
g	Acceleration of gravity, ft/s^2
GAC	Gulfstream Aerospace Corporation
GM	gain margin, decibels
GS	Gulfstream Aerospace Corporation implemented spike model
$\dot{h}$	vertical speed, ft/s
HQ	handling qualities
HUD	head-up display
K	represents 1,000 of a quantity

Kf	multiplier on baseline airplane aerodynamic look up
KIAS	knots indicated airspeed
Km	multiplier on spike aerodynamic coefficient
Ko	multiplier on spike model uncertainty bias
Lat-dir	lateral-directional
Max	maximum
Min	minimum
NASA	National Aeronautics and Space Administration
Ny	lateral acceleration, *g*
Nz	normal acceleration, *g*
Nza	slope of normal acceleration with respect to angle-of-attack, *g*/rad
P	roll rate, deg/s
PIO	pilot induced oscillation
PM	phase margin, deg
PRAD	pitch ratio adjust device
Ps	static pressure, lb/ft^2
Pt	total pressure, lb/ft^2
$\bar{q}$	dynamic pressure, psf
Q	pitch rate, deg/s
QS	Quiet Spike™
R	yaw rate, deg/s
$\dot{R}$	yaw acceleration, deg/s^2
RRAD	roll ratio adjust device
α	angle-of-attack, deg
β	angle-of-sideslip, deg
Δ	change in a parameter
ϕ	bank angle, deg
ω	frequency, rad/s
ω_{co}	cross over frequency, rad/s
ω_{sp}	short period frequency, rad/s
ω_{dr}	Dutch roll frequency, rad/s
ψ	true heading, deg
ζ	damping ratio
ζ_{dr}	Dutch roll damping ratio
ζ_{sp}	short period damping

INTRODUCTION

Independent studies have shown that a market exists for supersonic business jets (refs. 1,2). The Federal Aviation Administration (FAA) regulations that prohibit commercial aircraft from causing sonic booms over populated areas represent a significant challenge to aircraft designers working to produce supersonic civilian aircraft. Developing a technology to attenuate or "soften" the sonic boom of a supersonic airplane could enable the development of a new generation of supersonic civilian aircraft.

Quiet Spike™ is a technological concept developed by Gulfstream Aerospace Corporation (GAC) (Savannah, Georgia) as a method for softening the sonic boom for supersonic business jet-sized aircraft by attenuating the shock wave into a series of smaller shock waves across a telescoping spike extending from the front of an aircraft (refs. 3-6). The structural dynamics and load properties of such a spike extending from the front of an airplane, and its overall effect on the dynamic behavior of the airplane are not well known, especially in the transonic and supersonic flight regimes (refs. 7-10). The main program goal was to collect flight data to verify the spike structural dynamics and loads model up to Mach 1.8, and to validate the technical feasibility of a morphing fuselage (refs. 11-14).

The GAC partnered with the National Aeronautics and Space Administration (NASA) Dryden Flight Research Center (DFRC) (Edwards, California) to conduct flight tests of a GAC designed and manufactured half scale version of an extendable spike, which was attached to the nose of a NASA DFRC F-15B (McDonnell Douglas, now the Boeing Company, Chicago Illinois) (ref. 11). The spike was instrumented by NASA DFRC to collect data during ground and flight tests in a limited part of the F-15B flight envelope up to Mach 1.8 (refs. 8-11). NASA DFRC was also responsible for integration and flight-testing, which included ground tests, pre-flight and post-flight flight data analysis to ensure safety-of-flight during the envelope expansion. The analysis done by NASA DFRC covered the areas of air data calibration, aero servo-elastic clearance and structural dynamics, aerodynamics, and stability and control (ref. 11-13).

Limited aerodynamic modeling was accomplished by GAC, NASA DFRC, and Desktop Aeronautics Incorporated (DAI) (Stanford, California) to estimate the effects of the spike on aircraft stability (refs. 11, 12). Several modeling techniques including empirical data and Computational Fluid Dynamics (CFD) analysis were used, and initial predictions of the effects of the spike were generated. These predictions indicated that the spike would reduce lateral-directional stability between 3 and 5 percent in the subsonic flight regime, and between 3 and 24 percent in supersonic flight. A marginal reduction in pitch stability between 3 and 5 percent was predicted by aerodynamic models for the entire flight envelope. From a stability and control perspective, the potentially destabilizing effects of the spike on the lateral-directional aircraft dynamics, especially at supersonic flight conditions, was one major concern entering into the flight test portion of the program. The potential air-data effects, caused by the spike, posed another major concern.

The objective of this report is to document the stability and control analysis approach used to support the project flight readiness reviews and flight tests. The analysis covered the sensitivity of the stability margins, handling qualities, and maneuvering limitations of the F-15B Quiet Spike™ configuration due to aerodynamic variation. It had also been determined that the air-flow at the location of the air data probe and the angle-of-attack cone could be influenced by the presence of the spike (ref. 12). A sensitivity analysis of the effect of the sensor errors on stability and control was therefore considered warranted. The results of the analysis and the implications for the flight test program are presented. A sample of the actual flight data analysis is also presented as a preview to a more detailed presentation of the flight data results corresponding to the stability and handling qualities analysis during the envelope expansion. These results are presented in a to be published follow-on report (ref. 13).

AIRCRAFT GENERAL DESCRIPTION

This section briefly describes the F-15B test bed airplane and the Quiet Spike™ test article, which was mounted on the nose of the F-15B. Figure 1 shows the NASA DFRC F-15B airplane with the spike attached. The NASA F-15B is a high performance twin-engine (F100-PW-100) tactical fixed-wing jet fighter airplane with a maximum design Mach number of 2.5, and serves as a research test bed for various in-flight experiments. Installed instrumentation and telemetry systems provide onboard data recording and real-time control room monitoring capability (ref. 11).

QUIET SPIKE™ DESCRIPTION

The Quiet Spike™, shown in figure 2, consists of a 6 ft long nosecone fairing, an extendable spike (14.15 ft retracted, 24.31 ft extended), and interface attachment hardware. It attaches to the F-15B forward fuselage at the radar support bulkhead and weighs approximately 450 lb. An electrically powered cable and pulley mechanism extends, and retracts the boom (refs. 1, 4).

SIMULATION DESCRIPTION

The NASA DFRC F-15B simulation facility includes a fixed-base real-time pilot-in-the-loop six-degree-of-freedom simulation with standard stick and rudder pedal inceptors for pilot controls, HUD cockpit pilot flight instruments, and external real-time visual imagery. The simulation can be run real-time or faster than real-time in a remote software only batch mode as an engineering analysis tool. Simulation runs can also be scripted to facilitate automated analysis (ref. 15).

The simulation incorporated a validated aerodynamic model. Four research flights were conducted prior to installing the spike on the airplane to gather data to update the NASA DFRC F-15B baseline aerodynamic model, and to calibrate air data parameters on the airplane. The air data calibrations were performed for the production pitot-static tube, the alpha vane, and a supplementary beta vane. Aerodynamic updates were implemented as increments to the baseline aerodynamic model in the simulation to improve overall time history comparisons between the simulation and flight data. These efforts validated the simulation as an analysis tool for the anticipated spike flight conditions and regimes. References 11 and 12 offer a more detailed description of the airplane baseline aerodynamic model with updates.

QUIET SPIKE™ MODELS

To ensure conservative estimates of the aerodynamic uncertainties, three independently developed aerodynamic models of the spike were implemented into the DFRC F-15B simulation for stability and control analysis (ref. 12). A model representing the spike only was developed by GAC using an Euler CFD method, which also incorporated empirical corrections. A second spike only model was developed at the DFRC using an aerodynamic vortex lattice modeling method for a subsonic model, flat plate theory, and empirical cone-cylinder drag data for a supersonic model. A third model was developed by DAI using an Euler CFD method to model the full airplane as well as a full airplane-with-spike model. This final DAI spike model was extracted as a set of parameter deltas representing the difference between these two models. The differences between the three independently developed models were significant enough to motivate the inclusion of all three in the stability and handling qualities analysis. All three models were incorporated as additive delta values to the baseline F-15B aerodynamic model in the simulation. The

deltas were applied to the following parameters: C_{L_α}, $CD_{\alpha\beta}$, C_{m_α}, C_{n_β}, C_{y_β}. Spike effects on the damping derivatives were not modeled and effects on the roll axis dynamics were estimated to be negligible. The effect of the spike on the aircraft mass properties was also modeled and the aircraft center of gravity was not significantly altered by the spike. A build up approach in flight test was followed to check the validity of these models as the envelope was expanded. Reference 12 offers a more detailed description of these aerodynamic models, including derivation and flight validation.

F–15B CONTROL SYSTEM DESCRIPTION

The NASA DFRC F-15B control system consists of an integrated mechanical and electrical single string, analog control augmentation system (CAS) operating in parallel to command stabilators (deflected symmetrically for pitch and differentially for roll), ailerons, and rudders. Typical inceptors (stick and rudder pedals) are used for piloted control. The CAS is a single string system in each of the 3 axes: pitch, roll, and yaw. Each axis can be engaged or disengaged in the cockpit and is modeled as such in the simulation. No changes were made to the production aircraft control system during the program. Simplified descriptions of the NASA DFRC F-15B control system are shown in figures 3, 4, and 5. Longitudinal pitch control by symmetric stabilator position is shown in figure 3, lateral-directional roll control by aileron and differential stabilator deflections is shown in figure 4, and lateral-directional yaw control by rudder deflection is shown in figure 5.

Mechanical pitch control is achieved mainly through a pitch ratio adjust device (PRAD) (fig. 3). This mechanical device automatically adjusts the gain on the stick path based on static and total pressure to provide desirable stick force per *g*. The only other feedback to the mechanical system is normal acceleration, which is used to trim the stabilator to a commanded *g* from the stick input. The pitch CAS (fig. 3) provides closed-loop control of blended aircraft acceleration and pitch rate, commanding the equivalent of normal acceleration in up-and-away flight and providing Level 1 handling qualities. When the landing gear is down, the normal acceleration feedback is bypassed and the system provides pitch rate command. The pitch CAS also utilizes angle-of-attack feedback to induce a stall inhibitor when a certain angle-of-attack is reached.

The primary mechanical roll control system, shown in figure 4, contains the roll ratio adjust device (RRAD), and is augmented with a CAS. Similar to the PRAD, the RRAD varies the gain on the stick path based on calibrated airspeed when Mach is greater than 1. The roll CAS provides closed loop control of aircraft roll rate. A roll CAS command limiter is scheduled with calibrated airspeed and angle-of-attack to reduce structural loads on the differential stabilator, and provide compatible high angle-of-attack differential stabilator control with the mechanical roll control system.

The mechanical yaw control system, shown in figure 5, illustrates the aileron to rudder interconnect (ARI), and the connection between the rudder pedal and the rudder. The ARI commands rudder deflections in response to lateral stick inputs, with the lateral stick-to-rudder control surface deflections scheduled via the mechanical system symmetric stabilator. The ARI is only operative for Mach below 1.0; otherwise the ARI output is zero. The yaw CAS provides closed loop control of blended aircraft lateral acceleration and yaw rate to augment Dutch roll damping and turn coordination. Roll coordination is achieved by a roll-to-yaw cross feed scheduled with angle-of-attack. The roll-to-yaw cross feed is nullified above Mach 1.5.

SIMULATION ANALYSIS

Three main stability and control issues were identified for analysis as part of the airworthiness evaluation of the F-15B Quiet Spike™ configuration prior to the first flight. The issues identified for analysis included:

1. The effects of the spike induced aerodynamic changes on the F-15B airplane flight dynamics,

2. The effect of the spike induced airflow on the air data and angle-of-attack sensors, and implications for flight dynamics,

3. The potential unfavorable flight dynamic effects during failure modes.

Failure mode analysis was conducted, but will not be addressed in this report. Other issues such as sideslip crosswind landing limits, minimum control speed, and stabilator trim authority were evaluated, deemed inconsequential, and not covered in this report. The primary focus of analysis was on the pitch and yaw axis. Early aerodynamic model estimates indicated that the roll axis was not significantly affected by the presence of the spike. Figure 6 shows the Quiet Spike™ design envelope and the conditions at which simulation analysis was performed.

The primary objective of the analysis was to evaluate the robustness of F-15B Quiet Spike™ stability and flying qualities to aerodynamic uncertainties. These uncertainties incorporated baseline F-15B aerodynamic model uncertainty, as well as spike aerodynamic uncertainty (ref. 12). The test approach, test conditions, aerodynamic uncertainties, and evaluation metrics that were used in the analysis are described below.

Approach

The analysis was accomplished in an automated batch fashion by developing two simulation software tools: a simulation run tool and a linear analysis tool. The run tool generated nonlinear simulation response time histories, and linear aerodynamic models at various conditions and configurations. The analysis tool validated the linear models, and calculated the parameters of stability and handling qualities based upon the linear aerodynamic models and other models generated from the simulation run-tool.

The simulations generated time history responses to a doublet input in all three axes for 12 aerodynamic stress cases. The time histories also incorporated combinations of several different vehicle configurations and multiple flight conditions. For each aerodynamic stress case, the aerodynamic uncertainties of the spike and baseline F-15 model were varied in a worst-case direction. This method was implemented to assess the stability robustness of the models, and to characterize instabilities and degraded handling qualities. The stress cases are discussed in detail in the next section. Fifteen flight conditions within the Quiet Spike™ envelope were evaluated, including one point in the power approach configuration (fig. 6). The simulation test cases evaluated the nominal aerodynamics and aerodynamic stress cases for both CAS-on and CAS-off; 3 different fuel weights; and all 3 spike aero models with the spike fully extended, and to a limited degree with the spike fully retracted. The simulation run was paused in a trimmed state prior to the doublet being executed to generate a linear aerodynamic model for each test case.

The linear analysis tool consisted of nonlinear Simulink® (The MathWorks, Natick, Massachusetts) versions of the FORTRAN control system and actuation models. This tool integrated these Simulink® control actuation system models with the linear aerodynamic model generated by the nonlinear simulation for each test case, and then generated a linear model of this integrated model. The tool also determined

the parameters of the stability and handling qualities from the linear integrated models for each analysis case, and flagged any cases that violated predefined criteria of the stability and handling qualities. Additionally, the tool flagged predefined maneuver limit violations.

The linear models were validated for each test case by comparing the time histories to those generated by the nonlinear simulation. Figures 7 and 8 compare time histories of the linear and non-linear nominal airplane simulation for the pitch and yaw axis respectively at an altitude of 45,000 ft at Mach 0.8, CAS on. Pitch and yaw CAS off comparisons of the same configuration at the same condition are shown in figures 9 and 10 respectively. The comparisons shown were made with 8,000 lb fuel loading. These comparisons, typical of all configurations and conditions evaluated, indicated good comparisons between the linear models and the nonlinear simulation.

The run tool generated response time history data and linear aerodynamic models for over 24,000 run cases for the combined subsonic, transonic, and supersonic analysis phases. The analysis tool evaluated all the run cases generated by the run tool. Analysis cases that were flagged by the analysis tool for violation of handling qualities criteria were used to define critical flight conditions and configurations. The worst cases among those flagged were selected for further investigation by pilot-in-the-loop simulation exercises. The flagged cases were also used to define ranges of acceptable uncertainty on aerodynamic model parameters as a measure of the stability robustness of the aircraft and spike configuration.

Aerodynamic Stress Cases

Aerodynamic stress cases that were used in the analysis are described in table 1. The numbers in table 1 represent multiplicative factors Kf, 0, or -1 on uncertainties in the aerodynamic parameters. Equation 1, the equation for the rolling moment due to aileron deflection, $C_{l_{da}}$, illustrates how a multiplicative factor, Kf in this case, was used to modify the baseline aerodynamic model uncertainties:

$$C_{l_{da}} = C_{l_{da}}_\text{table} + \Delta C_{l_{da}} * Kf \tag{1}$$

$C_{l_{da}}_\text{table}$ is the value read from the simulation aerodynamic tables; $\Delta C_{l_{da}}$ is an uncertainty on $C_{l_{da}}$ based on the baseline F-15B flight test data, and is tabulated in the simulation as a function of Mach; and Kf is a multiplier on that uncertainty. Thus, a factor of 1 in table 1 indicates that the full uncertainty was applied to the associated parameter.

The spike model aerodynamic uncertainty is modeled with a multiplier Km and an offset (or bias) uncertainty. Equation 2, the equation for yawing moment due to the spike, $C_{n_{SPK}}$, illustrates the usage:

$$C_{n_{SPK}} = Km * C_{n_{SPK}}_\text{table} + C_{n_{SPK}}_\text{offset} * Ko \tag{2}$$

The first element for $C_{n_{SPK}}$ in table 1 defines the Ko parameter, a multiplier on $C_{n_{SPK}}_\text{offset}$. The second element in the table is associated with the Km parameter, which is a multiplier on the magnitude of the $C_{n_{SPK}}_\text{table}$ data. Km varies between an uncertainty of K and 1 / K, where K is the multiplier on the nominal spike model, which covers the uncertainty observed in the data for a given spike model. The uncertainties, K, and offset values are tabulated in the simulation as a function of Mach number for a given spike model.

The Kf factor in table 1 is chosen to vary aerodynamic parameters in worse case directions. Cases 1-4 represent reduced pitch stability and reduced stabilator effectiveness. C_{L_α}, the lift curve slope, is reduced to allow increased trim angle-of-attack. The pitch control surface effectiveness is reduced to allow increased variation in stabilator positions, which influences some lateral-directional aerodynamic parameters. Cases 1 and 2 have the sideslip derivatives chosen for reduced directional stability. Note that the side force due to sideslip, C_{y_β}, factors into stability due to the lateral acceleration feedback in the control laws. Similarly, the total side force contribution of the spike, $C_{y_{SPK}}$, has Km and Ko chosen for reduced stability, as well as Km for $C_{n_{SPK}}$.

Case 1 represents the case where lateral-directional control surfaces have decreased effectiveness. Case 2 represents the case where lateral-directional surfaces have increased effectiveness. Cases 3 and 4 cover the combination of lateral-directional control surface effectiveness for increased directional stability. Cases 5 thru 8 are a repeat of Cases 1 through 4 except the trends in the pitching moment and lift derivatives are opposite, that is, the signs are reversed on the factors associated with those derivatives.

Cases 9 and 10 both exhibit reduced directional stability and reduced control surface effectiveness. Case 9 provides reduced pitch stability and increased stabilator effectiveness, and case 10 provides increased pitch stability and reduced stabilator effectiveness. Case 11 is a repeat of case 1, except the sign of the C_{L_α} gain is changed for an increased lift curve slope, which will effectively destabilize the airplane by increasing the gain in the normal acceleration feedback path of the controls laws. Similarly, case 12 is a repeat of case 5, with the exception of the changed C_{L_α} gain to the stabilizing direction.

Evaluation Metrics

Metrics utilized in evaluating the simulation data are presented for both the automated linear batch analysis and the follow-up non-linear piloted simulation analysis.

Linear Analysis Metrics

Linear analysis metrics in the areas of stability margins, handing qualities, sideslip limits based on loads, *g*-limits, and stabilator trim requirements were defined for the nominal and the stress cases. Table 2 defines stability margin metrics for the nominal case and the stress cases. These margins were derived by engineering judgment based on previous flight test experience, and were the same for the spike extended and retracted cases.

The CAS off stability metric was determined by checking closed loop roots on the right half of the complex s-plane for the bare-airframe model. It was considered a more direct and intuitive way of estimating the stability of the bare-airframe model in the CAS off scenario than stability margins. The CAS off stability was evaluated due to the CAS being a single string system, and switching the CAS off was defined as a procedural mitigation in the event of an aerodynamic-structural excitation occurring in flight. The potential occurrence of an aerodynamic-structural excitation was a concern especially since aero-servo-elastic structural mode interaction characteristics were observed during ground tests.

The handling qualities metric values, of the airplane with the spike, had to meet Level 1 handling qualities or the same level as the baseline F-15B for the nominal CAS on case. For CAS on stress cases, the handling qualities metric values were required to be Level 2 or better. With the CAS off, the requirement was that the aircraft dynamics had to remain controllable. Figure 11 defines Level 1, 2, and 3 criteria from reference 16, which was used in the metric evaluations. These criteria are defined in terms of

the control anticipation parameter (CAP), the short period damping ratio ζ_{sp}, the Dutch Roll frequency ω_{dr}, and the Dutch Roll damping ratio ζ_{dr}. CAP is approximated as shown in equation 3:

$$\mathrm{CAP} = \omega_{sp} * \omega_{sp} / \mathrm{Nza} \tag{3}$$

where ω_{sp} is the short period frequency, and Nza is the slope of normal acceleration with respect to angle-of-attack.

Since gross, fighter-like maneuvering was not required for the Quiet Spike™ program, criteria applicable to approach and landing task, which are suitable for tasks involving precision, were used in the evaluation process. Fighter class vehicle considerations were applied (ref. 16).

Flight Maneuvering Limits

The spike design limits set several aircraft flight test limits (ref. 11). The limits discussed here were directly relevant to the analysis of the stability, control, and handling qualities. The design limit load factors for the spike resulted in -1.5 *g* to 5 *g* normal aircraft acceleration, and +/- 3 *g* lateral aircraft acceleration limits. An additional flight dynamic limit, based on previous F-15B flight test fixture design and flight test experience, was a sideslip multiplied by dynamic pressure ($\beta\bar{q}$) of 5,500 deg • psf. Angle-of-attack limits of 12 deg for up-and-away flight and 15 deg during powered-approach were set primarily to mitigate potential structural mode interaction at high angles-of-attack issues that were identified during ground tests. Additional flight-dynamic guidelines for intentional flight maneuvering were set at 3,000 deg • psf and 3 *g* normal acceleration to mitigate sudden, short duration dynamic excursions that could violate the limits (ref. 11). Limits were established for both nominal and stress cases, and for CAS on and off. Bank angle limit considerations were based on reduced *g* and angle-of-attack envelopes. These limits are shown in table 3.

Non-linear Pilot–in–the–loop Simulation Evaluation Tasks and Metrics

Pilot-in-the-loop simulation evaluation tasks for up-and-away configurations began with pitch-roll-yaw doublets followed by a 3 *g* turn with the CAS on; the CAS was switched off while in the turn. The pilot was then required to return the airplane to wings-level and initiate a constant altitude deceleration to 250 knots followed by a pitch-roll-yaw doublet. For the powered approach configurations, the pilot evaluated the handling qualities during nominal approach, offset runway approach, and landing. For both powered approach and up-and-away configurations, pilot comments on controllability were obtained. The pilot-in-the-loop simulation response was also checked for compliance with predefined flight performance limits.

Pilot metrics included the aforementioned flight maneuvering limits as well as metrics based on pilot comments shown in table 4. Pilot comments for CAS on, for the baseline airplane model, and for the stress cases were required to fall within the constraints as shown in table 4. The constraints for all cases of CAS off are also shown in table 4. The same limits listed in table 3 were established for both nominal and stress cases, as well as for CAS on and off.

Test Conditions

The flight test conditions identified in figure 6 were analyzed with the batch simulation. These conditions represented the conditions of primary interest in the planned Quiet Spike™ flight envelope as shown in figure 6. The altitude of 15,000 ft at Mach 0.3 test condition was done in the power approach configuration with the gear and flaps down.

ANGLE–OF–ATTACK AND AIR DATA ERROR SENSITIVITY

It was determined that the airflow at the location of the air data probe and the angle-of-attack cone could be influenced by the presence of the spike (ref. 12). A sensitivity analysis of the effect of the sensor errors on stability and control was therefore warranted.

Angle–of–Attack Error Sensitivity

To evaluate the sensitivity of the turn coordination to errors in sensed angle-of-attack, a positive and negative error of two degrees was inserted into the angle-of-attack calculation in the simulation, and fed back into the control laws. An error of two degrees was selected as a large, but reasonable error to assume in the case of angle-of-attack based on previous flight test experience. The primary objective of the analysis was to evaluate the coordination of the rudder during lateral inputs. A two-inch lateral control stick doublet was input to the simulation at all test conditions below Mach 1.4. Evaluation was made for the nominal aerodynamics for each spike model and the baseline airplane model. Both pitch CAS on and off configurations were analyzed in this way.

Air Data Error Sensitivity

The flight control system in the pitch axis uses the Pt/Ps ratio and Pt–Ps quantity from the total and static pressures to set the stick gain. The spike would change the airflow at the air data probes and modify the stick gain from the baseline value at a given condition. If this distortion was significant, it could conceivably have led to a pilot induced oscillation (PIO) tendency or degraded handling qualities.

Five of the up-and-away subsonic flight conditions were selected for the stress analysis. The Ps and Pt errors were introduced into the simulation, which resulted in an equivalent 10% error in altitude and Mach number. The error criterion was based on engineering judgment from previous flight test experience. Time histories of doublets with and without the error were generated in batch simulation runs to gauge the sensitivity of the stick gain. For transonic and supersonic conditions, the air data sensitivity was evaluated with piloted simulation of the pitch ratio gain fixed at the minimum and maximum values. This approach represented a failure mode, but also encompassed the spike flow induced air data error scenario. Although primary interest was in the CAS on evaluation, analysis was also done with the CAS off at some of the conditions. All evaluations were made with the spike extended.

ANALYSIS RESULTS

This section documents the results of the pre-flight airworthiness evaluation of the F-15B Quiet Spike™ airplane. The analysis is presented with the spike extended. Results of the analysis with the spike retracted showed that the effect on the stability and handling qualities characteristics were either similar to or more benign than the extended spike case. The analysis was conducted in two phases. The first phase of the analysis was conducted at the conditions specified in the test plan up to the Mach 0.8 flight condition in an effort to begin the flight test clearance of the subsonic envelope, while the second phase of the analysis was conducted for the transonic and supersonic envelope.

Subsonic Aerodynamic Stress Analysis

This section documents the results of the stress analysis for the flight regime below Mach 0.8 flight. This discussion emphasizes where evaluation metrics were flagged and examines subsequent piloted

simulation results that were performed to further investigate the flagged cases. Approximately 5,880 analysis cases were generated in this subsonic analysis phase.

Pitch Axis

The results of the pitch analysis are described here. Three different fuel loading conditions: heavy, medium, and lightweight were implemented for C.G. (center of gravity) variance. Combinations covering these three fuel weights, five flight conditions, CAS on and off configurations, baseline F-15B airplane, the F-15B airplane with the baseline airplane and three boom-aero-models, boom retracted and extended configurations, and six stress cases were analyzed. Stress cases 2 to 4 described in table 1 are identical to case 1 for the pitch axis uncertainty variations, and similarly cases 6 to 8 are identical to case 5; only case 1, 5, 9, 10, 11, and 12 were analyzed for the pitch axis.

In the pitch axis analysis, no stability margin metric violations were flagged for the stress analysis for all configurations and conditions tested. The CAS on cases indicated that an ample stability margin existed. Figure 12 shows typical gain and phase margins at an altitude of 15,000 ft, at Mach 0.8 with 8,000 lb of fuel weight. Figure 12 also compares the various uncertainty cases and spike models, with the asterisk indicating the data point of the nominal F-15B airplane without the spike. Despite the worst case aerodynamic variations, the minimum gain margin was around 14.5 dB, and the minimum phase margin was around 70 deg. For the pitch CAS off cases, the airframe stability roots indicated a small number of conditions at Mach 0.8, which exhibited an unstable phugoid mode. The frequency of the mode was typically quite low, around 0.5 rad/sec, which was deemed to be well within the pilot's ability to compensate and thus not an issue of concern.

None of the handling qualities CAP and damping metrics were violated in the analysis for either CAS on or CAS off. Some CAS off cases caused the airplane to dip into Level 3 in the CAP and damping. The worst of these Level 3 cases occurred for the Gulfstream spike model with 2,000 lb of fuel weight. The lowest damping occurred for stress case 9 at an altitude of 45,000 ft at Mach 0.8 (fig. 13). The lowest CAP occurred for stress case 11 at an altitude of 15,000 ft at Mach 0.8 (fig. 14). These conditions were identified for piloted simulation evaluations. For powered approach configuration, a Level 2 damping result was the most degraded handling qualities case. Although not expected to be a problem in flight, the case was identified for evaluation with the piloted simulation to determine the sensitivity of the damping parameter with respect to the 5 fps touch down limit.

Three of the pitch CAS off test cases exhibited small excursions above the angle-of-attack metric criteria. Although not considered significant (the worst case was 0.5 degrees over the 12 degree limit), the case was included in the piloted simulation evaluation to verify that piloting tasks could be achieved without exceeding the limits. This case was identified as stress case 9 at an altitude of 45,000 ft at Mach 0.8, Gulfstream spike model with 8,000 lb fuel weight.

CAS off run cases were flagged for normal acceleration excursions outside the minimum criteria. For the most part, these excursions were slightly under the 0 *g* limit. A few of the runs, however, showed excursions to -0.5 *g* to -1 *g* (fig. 15). The worst of these cases, identified to be at an altitude of 15,000 ft, at Mach 0.8, Gulfstream spike model, stress case 9, and 2,000 lb fuel, was tested in the piloted simulation.

The pilot-in-the-loop simulation was the final test to resolve any potential concerns raised by the flagged test cases for the pitch axis, subsonic, analysis. Five cases were identified as worst cases that were fully representative of all flagged cases, for further evaluation in the piloted simulation. These cases are summarized along with the lateral-directional cases in table 5.

Lateral–Directional Axis

This section describes the result of the subsonic lateral-directional analysis. Heavy, medium and light weight fuel loadings were used for C.G. variance. Yaw and roll doublets were generated separately and analyzed for all combinations of three fuel weights, five flight conditions, CAS on and off configurations, baseline F-15B airplane and three spike models, spike retracted and extended configurations, and all twelve stress cases.

The CAS on cases exhibited ample stability margin. The test case exhibiting the lowest margin in the directional axis occurred at an altitude of 15,000 ft, at Mach 0.8, however, it did not violate the minimum stability criteria. The gain margin at this point was approximately 10 dB and the phase margin was approximately 49 degrees. For the CAS off cases, there were several bare-airframe stability cases flagged. The worst cases among these at each flight condition were checked in the piloted simulation. The worst-case time-to-double-amplitude of these cases was 3.465 seconds, which did violate the damping ratio criteria.

All of the CAS on cases exhibited Level 1 handling qualities. The CAS off cases yielded several cases with Level 3 handling qualities for all three of the fuel weight conditions at an altitude of 45,000 ft, at Mach 0.8. One case at the mid-fuel weight condition exhibited a slightly negative damping ratio. This case was checked in the piloted simulation. For all other flight conditions and fuel weights, the handling qualities for the CAS off scenario were Level 2 and Level 1.

There were several minimum and maximum Nz limit violations at each fuel weight condition. The 2 worst cases exceeded -1 g and 5 g and these cases were checked in the piloted simulation. In the batch simulation checks, it was determined that the worst case Nz violations, which occurred across all fuel weights were induced by a combination of the Gulf Stream spike model and the uncertainties of stress case 2.

There were a handful of $\beta\bar{q}$ limit violations around 6,000 deg • psf in the batch analysis across all fuel weights. These cases all occurred at an altitude of 15,000 ft, at Mach 0.8 and were all induced by uncertainty cases 2 and 6 even in the baseline simulation (i.e. with no spike). These cases were identified for evaluation in the piloted simulation. There were ϕ limit violations at each flight and fuel weight, and the worst cases were also checked in the piloted simulation.

Piloted Simulation

Table 5 presents a list of all the piloted simulation evaluations conducted for the subsonic envelope to Mach 0.8, combining the results of the pitch and lateral-directional axis analysis where further piloted evaluation was required. In table 5, GS, DTA, DFRC and BL refer to the spike aerodynamic models developed by Gulfstream Aerospace Corporation, Desktop Aeronautics Incorporated and Dryden Flight Research Center respectively with the base-line model.

Piloted simulation results for the nominal airplane and the three spike models with uncertainties, in the CAS on configuration indicated that the handling qualities of the F-15B Quiet Spike™ configuration were satisfactory without further improvement. For the power approach cases, pilot comments indicated that controllability of the airplane was easily maintained. There were no problems maintaining the approach and landing within the established metric limits. No surface saturation was observed. The highest sink rate at touchdown recorded in the simulation analysis was near 5 fps, but it was noted that the fixed based simulation and visual graphics environment made it harder for the pilot to estimate and maintain sink rate on approach. Controlling sink rate at touchdown was considered to be significantly easier in the real airplane compared to the simulation.

For the up and away configurations, pilot comments on three of the pitch CAS off cases indicated the responses were lightly damped, but easily controllable. With these cases, mild pilot induced oscillation tendency was noted for stress case 9 at an altitude of 15,000 ft, at Mach 0.8. All other metrics were maintained.

The CAS off, lateral-directional cases in the up and away configurations were determined to be controllable despite some undesirable characteristics. The pilot commented that the case, which exhibited negative Dutch roll damping at an altitude of 45,000 ft, at Mach 0.8 flight condition was undesirable, but that the Dutch roll frequency was low enough to be manageable with pilot-in-the-loop control. However, some of the cases at high dynamic pressure (fig. 16) elicited highly undesirable pilot comments due to high frequency, lightly damped responses. Sideslip induced roll required continual application of lateral stick to damp out. By decelerating to 250 KIAS, the frequency was decreased and the dynamics became acceptable. Therefore this approach was defined as mitigation during the flight test. The cases evaluated for bare airframe stability issues were determined by the pilot to be objectionable, but controllable.

In general, the pilots were able to avoid violations of maneuvering limits by conservative application of control inputs. At an altitude of 15,000 ft, at Mach 0.8, two of the cases evaluated in the piloted simulation exceeded the $\beta\bar{q}$ limit of 3,000 deg • psf by about 600 deg • psf. Subsequent repeats of these cases with the pilot using more conservative inputs resulted in no violations. Other metrics were maintained within limits, but some differentiating of results was required based on aggressive pilot inputs performed for evaluation purposes. These aggressive pilot maneuvers would, in some instances, cause Nz, angle-of-attack, and $\beta\bar{q}$ metric criteria violations that did not occur under normal maneuvering conditions. No issues were observed relating to normal acceleration or bank angle sensitivity.

Transonic and Supersonic Stress Analysis

The results of the transonic and supersonic analysis covered the flight conditions from Mach 0.8 to Mach 1.8, and are presented in this section. More than 18,000 transonic and supersonic simulation check cases were generated at the ten flight conditions higher than Mach 0.8. Heavy, medium, and lightweight fuel loadings were used for C.G. variance. Every combination covering the three fuel weights, ten flight conditions, CAS on and off configurations, baseline F-15B, the F-15B involving three spike models with spike retracted and extended configurations, and twelve uncertainty cases was analyzed.

Pitch Axis

Table 6 summarizes the cases with metric limit violations in the pitch axis analysis. Adequate stability margin was observed for all pitch CAS on cases in the transonic and supersonic flight regime for all configurations. Typical gain and phase margins are shown in figure 17 at an altitude of 45,000 ft, at Mach 1.8 condition. Figure 17 compares the various uncertainty cases and spike models, with the asterisk data point indicating the nominal F-15B airplane without the spike. The worst cases in terms of stability at this condition exhibited approximately a 16 dB gain margin and approximately a 75-degree phase margin. For the pitch CAS off cases, there were a small number of conditions that violated the bare-airframe stability criteria and also exhibited an unstable phugoid mode. The unstable phugoid mode was also observed in the baseline F-15B airplane and the frequency was typically low. The four worst phugoid mode cases were identified for evaluation in the piloted simulation.

No CAP handling qualities criteria violations were observed in the analysis for CAS on and pitch CAS off. However, numerous damping criteria violations were observed in the pitch CAS off configuration. The lowest damped case, ζ = 0.039, was observed in the transonic flight region at an altitude of 49,000 ft, at Mach 1.1 in the heavy fuel, uncertainty stress case 9, F-15B without the spike

configuration. A simulation response time history comparison of all stress cases at this flight condition is shown in figure 18. It can also be seen in figure 18 that even the baseline F-15B response (shown in the light orange shade) is lightly damped. Although the low damping conditions were also observed in the baseline F-15B, ten of these low damping cases were identified based on engineering judgment for evaluation in the piloted simulation.

Numerous CAS off cases were flagged for minimum Nz excursions. These excursions were for the most part just under the 0 *g* minimum criteria. A few cases showed excursions to -0.5 *g* (fig. 19). The six worst Nz excursions were identified for further evaluation in the piloted simulation. In summary, twenty cases were identified for further evaluation in the piloted simulation for the pitch axis.

Lateral–Directional Axis

The number of cases with metric limit violations in the lateral-directional axes analysis is summarized in table 7. Full aerodynamic uncertainty variations were applied to flight conditions up to and including Mach 1.4. Due to inadequate stability margins at Mach 1.6 to 1.8, the aerodynamic uncertainty variations were reduced to ¾ of the original values for flight conditions higher than Mach 1.4. Reducing the aerodynamic uncertainty variations imposed narrower uncertainty tolerances around the critical aerodynamic parameters that would be applied during post flight parameter estimation (ref. 13) for further flight envelope clearance. Adequate stability was observed for all test cases across the transonic and supersonic flight regime for the CAS on and off, and all spike models and configurations after the aerodynamic uncertainties were reduced. Typical gain margins for the test cases were typically above 20 dB and the phase margins were above 65 degrees.

Handling qualities metric violations were not found for CAS on in all three axes, or CAS off in roll or yaw axis up to Mach 1.4. Stress cases with full uncertainties were applied at Mach 1.6 and 1.8 and resulted in several low to negative Dutch roll damping values. However, after applying the reduced uncertainty levels at these Mach numbers no handling qualities violations were found.

A few handling qualities metric violations were flagged for the CAS off runs with regard to Nz excursions outside the established boundary. These excursions resulted from cross coupling effects from uncertainty stress cases with yaw and roll doublets. The excursions were limited to $-0.73 \leq Nz \leq 4.4\ g$. The worst Nz excursions were identified for further evaluation in the piloted simulation. A small number of ϕ limit violations were found at an altitude of 18,000 ft, at Mach 0.95 for the three fuel weights tested. The worst of these cases were also evaluated in the piloted simulation. Numerous test cases exceeded the 3,000 deg • psf $\beta\bar{q}$ limit. These violations were induced by stress cases 2 and 6, even in the baseline simulation with no spike. The largest violations occurred at the Mach 0.95, and altitude of 18,000 ft transonic condition. Fifteen test cases were identified, which covered the lateral-directional axis concerns, for pilot in the loop simulation evaluation.

The worst-case metric limit violations identified for evaluation in the real time simulation by the two project pilots are shown in table 8. These violations included pitch trim, Nz sensitivity, $\beta\bar{q}$, rolling tendency, bare-airframe stability, and short period damping.

Piloted Simulation

Piloted simulation evaluation covered flight conditions in the transonic and supersonic flight regime, baseline F-15 aerodynamic model, the three spike models, two fuel loadings, eight of the twelve aerodynamic uncertainty stress cases, and spike configuration in both extended and retracted position for all three axes.

Numerous Nz, $\beta\bar{q}$, and Ny limits were exceeded during the piloted simulation evaluations. All of the violations were due to excessive pilot inputs and were not considered valid violations. In these cases, the pilots were evaluating controllability with control inputs much greater than what would be expected in flight test maneuvers. Despite the aggressive pilot inputs, the aircraft was still controllable. During the recovery portion of the task, none of the limits on any parameters were exceeded. The consensus of the two evaluation pilots was that with the CAS engaged the handling qualities were not degraded significantly. However, with the CAS off in all axes the handling qualities were significantly worse, especially at supersonic speeds. Even with the poor handling qualities, the airplane was still controllable at supersonic speeds and safe deceleration to the subsonic envelope was still possible.

Angle–of–Attack Error Sensitivity

Analysis across all flight conditions indicated that pitch-roll coordination was affected by sideslip inducing alpha excursions, which would in turn induce Nz transients. These effects, however, were not significantly adverse. Regardless of the pitch CAS state, the peak transients in the simulation response during the lateral-directional doublet showed no appreciable difference when a 2 and -2 degree error in angle-of-attack was added. The characteristics of the transients varied, but the peak values were generally similar. Worst-case transients occurred at the higher dynamic pressure conditions.

An example of the effect of the error in angle-of-attack at an altitude of 15,000 ft, at Mach 0.8 using the Gulfstream spike model is shown in figures 20 and 21 for the pitch CAS on, and in figures 22 and 23 for the CAS off. The green trace shows the -2 degree error, and the blue trace shows the +2 degree error. For the pitch CAS on, the normal acceleration traces are similar in shape with about a 0.3 *g* difference in peak. Similar characteristics are observed for the pitch CAS off results. Peak transients for the CAS off appear larger than the pitch CAS on results. And the +2 degree error transient has a larger peak. These results were deemed acceptable and alleviated the concern over the potential negative effect of an angle-of-attack data error on the stability and handling qualities.

Air Data Error Sensitivity

By observation of how the static and total pressure errors affected the control stick gain in the control laws, the worst case of the 6 subsonic conditions was determined to be at an altitude of 15,000 ft, at Mach 0.55. Overall the stick gain changed by approximately 15% due to the error at that condition. The time history comparison of aircraft responses of the nominal airplane and the airplane with the +/- 10% errors at an altitude of 15,000 ft, at Mach 0.55 is shown in figure 24. Little sensitivity was observed based on the air data error. For the transonic and supersonic conditions, piloted evaluations of the minimum and maximum pitch ratio gain revealed no problems with handling qualities when the CAS was on. With the CAS off, evaluations of minimum pitch ratio gains produced significantly reduced pitch stick authority resulting in marginally controllable handling qualities. Although not desirable, this finding was carried as an accepted risk.

FLIGHT TEST IMPLICATIONS

One major component of the flight test program was stability and control clearance of the F-15B Quiet Spike™ configuration. This section discusses the implications of the analysis results in terms of the flight test clearance restrictions and procedures.

Stability and Control Flight Test Clearance

The stress analysis displayed regions of aerodynamic variations on key derivatives, which resulted in acceptable stability margin, handing qualities, and flight dynamics regardless of the CAS state. To accelerate the envelope expansion flight-testing, each of the key nominal F-15B aerodynamic derivatives were plotted against Mach number.

Acceptable aerodynamic variation evaluated in the spike extended stress analysis was superimposed on the nominal derivatives to form regions of acceptable variation. Spike extended analysis variations were used because the retracted analysis indicated nearly the same or more benign results. Post-flight parameter estimation of the aerodynamic derivatives from flight tests over-plotted on these figures allowed a quick evaluation on whether those conditions were cleared, and whether subsequent expansion points were cleared. If the flight estimated derivatives fell within the regions of variation, then the F-15B Quiet Spike™ would be within acceptable variations as pre-determined by the analysis. If the trends observed as a function of Mach number projected that subsequent Mach number expansion points fell within the regions, then the F-15B Quiet Spike™ would be cleared to collect expansion test data at those points. If the projected trends indicated that an aerodynamic derivative fell outside its region, then further analysis would be warranted before it could be cleared to collect expansion test data. Figures 25 to 30 show the key up-and-away aerodynamic derivatives as Mach number varies up to 0.8 with the nominal F-15B shown as a dashed line, and the regions of variation shown as a solid line. Figures 31 to 36 show the key aerodynamic derivatives as Mach varies from 0.8 to 1.8. Note that from Mach 1.4 to 1.6, the uncertainty bounds narrow from the full uncertainty variation to three-fourths of the uncertainty variation. The reduced tolerance of aerodynamic variation was motivated by the reduction in stability margins observed with full uncertainties in the supersonic lateral-directional stability analysis at Mach 1.6 and Mach 1.8. For Mach numbers where stress analysis was conducted at two different altitudes (fig. 6), the most restrictive variation was used in the generation of the borders.

Post flight aerodynamic parameter estimation data were compared on these parameter uncertainty bounds after each flight to assess the stability and control of the F-15B with the spike configuration for the next test point. This data is discussed in more detail in the follow on report (ref. 13). Figures 37 and 38 show two examples of the parameter estimation plots and the projected trend analysis of C_{m_α} and C_{m_q}.

Another key aspect of the flight test clearance was the validity of the simulation. The simulation was the key tool in determining whether the aerodynamic variations observed in figures 25 to 36 were acceptable or not. If the simulation was not representative of the flight data, then the basis for determining acceptability of the aerodynamic variations was in question. Therefore, reasonable simulation comparisons with flight data were necessary to the envelope expansion process (ref. 13).

While the majority of the flight-test expansion and data collection process was done with the CAS on, clearing the envelope for the CAS off was important because the CAS is a single string system. Also, structural mode interaction ground tests had resulted in near zero margin for certain flight conditions, and it was decided that the best mitigation for such an occurrence in flight would be to turn the pitch CAS off. Although parameter estimated flight data would be compared to figures 25 to 36 for the CAS off considerations, the analysis results indicated no concerns for the CAS off dynamics for Mach numbers below Mach 0.8. To increase confidence in the CAS off dynamics, it was planned to collect data with the CAS off at a limited number of flight conditions below Mach 0.8. To evaluate the CAS off dynamics during flight tests, acceptable regions of the time-to-half amplitude, and the short period and Dutch roll mode were generated from the acceptable aerodynamic CAS off extended spike stress cases. These parameters plotted against dynamic pressure for three fuel weights in figures 39 to 42, formed a region where estimates from flight tests would be expected to fall. For the transonic and supersonic flight

conditions, the process of turning the CAS off to do the testing was deemed to have more risk than benefit, and the comparisons of the parameter estimated data in figures 25 to 36 would be relied on.

Flight Restrictions

Piloted simulation studies indicated that the CAS off damping in the yaw axis was highly oscillatory, and especially undesirable in the transonic and supersonic regions. Therefore, in the event of a CAS off situation, a procedure was established to maintain wing level and decelerate to a safe region of less than 250 knots, which would be well within Mach 0.8 or less. An additional constraint was placed on the pilot to minimize maneuvering during the deceleration. These restrictions were implemented as emergency procedure addendums.

CONCLUSION

The primary objective of the Quiet Spike™ flight research program was the aerodynamic, structural, and mechanical proof-of-concept of a large multi-stage telescoping nose spike installed on the front end of the NASA Dryden Flight Research Center F-15B aircraft. In the area of stability and controls, the primary objective was to assess the effect of the spike on the stability, controllability, and handling qualities of the airplane; and to develop an envelope expansion approach to maintain safety of flight. The two main issues were the uncertainty of the spike influenced aerodynamics on the flight dynamics of the F-15B airplane, and the implications for the airplane flight dynamics due to spike induced air flow in the vicinity of air data and angle-of-attack sensors. This report described the simulation analysis of these stability and control issues and the flight test implication based on the analysis.

Aerodynamic uncertainties on the nominal F-15B and the spike aero model coefficients were applied as worst case sets in automated simulation runs across several flight conditions, fuel weights, and control system configurations to evaluate the robustness of the system. Stability, handling qualities, and maneuvering limits were evaluated, and worst-case combinations that were flagged as violating criteria were further evaluated with pilot-in-the-loop simulation evaluations. As a result of the analysis, ranges of acceptable aerodynamic variations were formulated. These variations were used as guidelines for determining acceptable variations of parameter estimation from flight data during the F-15B Quiet Spike™ envelope clearance flight tests. With respect to spike induced airflow variations, sensitivity studies on the affects of air data and angle-of-attack miscalibrations due to the spike-influenced aerodynamics did not result in major concerns for the flight test.

Analysis was performed in two phases. The first phase of the analysis addressed the subsonic flight condition up to Mach 0.8. The second phase addressed the transonic and supersonic intended flight conditions up to Mach 1.8.

For the subsonic analysis, longitudinal stability margins for CAS on and CAS off configurations were generally adequate. An unstable low frequency phugoid mode, well within the pilot's ability to compensate, along with a tendency to dip into Level 3 in CAP and damping was discovered for the pitch CAS off configuration.

Lateral-directional stability margins were also generally adequate for the CAS on configuration. The CAS off configuration yielded several cases of reduced stability and several cases with Level 3 handling qualities as well as one negatively damped case. These cases were cleared in piloted simulation sessions. All other analysis cases yielded Level 1 and Level 2 handling qualities.

For the transonic and supersonic analysis, longitudinal stability margins were generally adequate for all of the CAS on configuration cases. For the CAS off configuration, a small number of bare airframe stability violations that also exhibited unstable phugoid modes were discovered. The unstable phugoid mode was also observed in the baseline aircraft, and the frequencies were typically low in both scenarios. Numerous cases of low damping were also discovered for the CAS off configuration. Any concerns over these dynamic characteristics were resolved through piloted simulation.

In the lateral-directional stability analysis, full aerodynamic uncertainties were only applied to analysis cases up to Mach 1.4 for acceptable stability. Stability margins were inadequate for conditions from Mach 1.6 to Mach 1.8 when full aerodynamic uncertainties were applied. Aerodynamic uncertainties were reduced to three-fourths their original values for analysis conditions higher than Mach 1.4 to ensure adequate stability margins for all analysis conditions for both the CAS on and CAS off configurations. The reduction of uncertainties during analysis was justified by imposing a markedly reduced tolerance for uncertainty in critical aerodynamic parameters during post flight parameter estimation after each flight test condition before clearing the next test condition in the envelope.

Analysis across all flight conditions indicated that pitch-roll coordination was adversely affected by sideslip inducing alpha excursions, which would in-turn induce Nz transients. However, these effects were not significantly adverse. Regardless of the pitch CAS state, the peak transients in the simulation response during the lateral-directional doublets showed no appreciable difference when a 2 and -2 degree error in angle-of-attack was added.

It was discovered that static and total pressure errors affected the control stick gain by as much as 15% in the control laws for some flight conditions. For the transonic and supersonic conditions, piloted evaluations of the minimum and maximum pitch ratio gain did not reveal any adverse handling qualities effects for the CAS on configuration. For the CAS off configuration, evaluations of minimum pitch ratio gains produced significantly reduced pitch stick authority resulting in marginally controllable handling qualities. Although not desirable, this finding was carried as an accepted risk.

Piloted simulation studies indicated that damping in the yaw axis was highly oscillatory, and especially undesirable for the CAS off configuration in the transonic and supersonic envelope regions. An in-flight procedure was established to maintain wings level and decelerate to a safe region of the envelope with minimal maneuvering in the event of a CAS off scenario.

TABLES

Table 1. Aerodynamic stress cases.

Coefficent	Case 1	Case 2	Case 3	Case 4	Case 5	Case 6	Case 7	Case 8	Case 9	Case 10	Case 11	Case 12
C_{m_0}	1	1	1	1	-1	-1	-1	-1	1	-1	1	-1
C_{m_α}	1	1	1	1	-1	-1	-1	-1	1	-1	1	-1
$C_{m_{dh}}$	1	1	1	1	-1	-1	-1	-1	-1	1	1	-1
C_{m_q}	1	1	1	1	-1	-1	-1	-1	1	-1	1	-1
C_{L_α}	-1	-1	-1	-1	1	1	1	1	-1	-1	1	-1
$C_{L_{SPK}}$	-1, 1/K	-1, 1/K	-1, 1/K	-1, 1/K	1, K	1, K	1, K	1, K	-1, 1/K	-1, 1/K	1, K	-1, 1/K
$C_{m_{SPK}}$	1, K	1, K	1, K	1, K	-1, 1/K	-1, 1/K	-1, 1/K	-1, 1/K	1, K	-1, 1/K	1, K	-1, 1/K
C_{y_β}	1	1	-1	-1	1	1	-1	-1	1	1	1	1
$C_{y_{da}}$	1	-1	1	-1	1	-1	1	-1	1	1	1	1
$C_{y_{dt}}$	1	-1	1	-1	1	-1	1	-1	1	1	1	1
$C_{y_{dr}}$	-1	1	-1	1	-1	1	-1	1	-1	-1	-1	-1
C_{l_β}	1	1	-1	-1	1	1	-1	-1	1	1	1	1
$C_{l_{da}}$	-1	1	-1	1	-1	1	-1	1	-1	-1	-1	-1
$C_{l_{dt}}$	-1	1	-1	1	-1	1	-1	1	-1	-1	-1	-1
$C_{l_{dr}}$	-1	1	-1	1	-1	1	-1	1	-1	-1	-1	-1
C_{l_p}	1	1	-1	-1	1	1	-1	-1	1	1	1	1
C_{l_r}	1	1	-1	-1	1	1	-1	-1	1	1	1	1
C_{n_β}	-1	-1	1	1	-1	-1	1	1	-1	-1	-1	-1
$C_{n_{da}}$	1	-1	1	-1	1	-1	1	-1	1	1	1	1
$C_{n_{dt}}$	-1	1	-1	1	-1	1	-1	1	-1	-1	-1	-1
$C_{n_{dr}}$	1	-1	1	-1	1	-1	1	-1	1	1	1	1
C_{n_p}	-1	-1	1	1	-1	-1	1	1	-1	-1	-1	-1
C_{n_r}	1	1	-1	-1	1	1	-1	-1	1	1	1	1
$C_{y_{SPK}}$	1, 1/K	1, 1/K	-1, K	-1, K	1, 1/K	1, 1/K	-1, K	-1, K	1, 1/K	1, 1/K	1, 1/K	1, 1/K
$C_{n_{SPK}}$	1, K	-1, K	1, 1/K	-1, 1/K	-1, K	1, K	1, 1/K	-1, 1/K	1, K	-1, K	1, K	-1, K

Reduced directional stability
Increased directional stability

Table 2. Stability margin metrics.

	CAS on		CAS off
	Nominal case	Stress cases	All cases
Gain margin	6 dB	4 dB	Real (Eigenvalue) < .01
Phase margin	45 deg	30 deg	

Table 3. Flight maneuvering limits.

Sideslip induced loads	$\beta\bar{q}$ < 3,000˚ psf
Normal acceleration	0 < Nz < 3.0*g*
Angle-of-attack	Up and away: -5˚ < α < 12˚
	Power approach: -5˚ < α < 15˚
Bank angle	Up and away: -60˚ < ϕ < 45˚
	Power approach: -45˚ < ϕ < 45˚
Sink rate at touch down	$\dot{h}$ < 5 fps

Table 4. Pilot comment metrics.

	Nominal case	Stress cases
CAS on	Satisfactory without improvement, or no worse than baseline F-15B	Objectionable, but control not in question
CAS off	Controllable	Controllable

Table 5. Piloted evaluation matrix.

Configuration	Condition altitude*/Mach	Spike model	Stress case	Pitch CAS	Yaw CAS	Fuel weight (lb)
Power approach	15,000/0.35	GS	10	Off	On	12,000
	15,000/0.35	GS	12	Off	On	12,000
	15,000/0.35	BL	1	Off	On	12,000
	15,000/0.30	DTA	10	On	Off	8,000
	15,000/0.30	BL	10	On	Off	8,000
	15,000/0.30	DTA	5	On	Off	2,000
Up and away	15,000/0.55	DTA	2	On	Off	8,000
	15,000/0.55	DTA	11	On	Off	8,000
	30,000/0.55	DTA	11	On	Off	8,000
	15,000/0.55	DFRC	2	On	Off	8,000
	30,000/0.55	DTA	2	On	Off	8,000
	45,000/0.80	DTA	9	Off	On	8,000
	45,000/0.80	GS	9	Off	On	2,000
	15,000/0.80	GS	11	Off	On	2,000
	15,000/0.80	GS	9	Off	On	2,000
	15,000/0.80	GS	2	On	Off	8,000
	15,000/0.80	GS	2	On	Off	8,000
	15,000/0.80	DTA	11	On	Off	8,000
	15,000/0.80	DTA	6	On	Off	8,000
	45,000/0.80	DTA	2	On	Off	8,000
	45,000/0.80	DTA	11	On	Off	8,000
	45,000/0.80	GS	11	On	Off	8,000

* Altitude (MSL)

Table 6. Pitch axis supersonic metric violations.

		Full uncertainty		
		Heavy fuel	Mid fuel	Light fuel
Pitch limits	Min α			
	Max α			
	Min g	X	X	X
	Max g			X
	Trim		X	X
Pitch HQ	CAP			
	ζ_{sp}	X	X	X
Pitch stability	GM			
	PM			
	BAS	X	X	X

Table 7. Lateral-directional supersonic metric violations.

		Full uncertainty			Full uncertainty to Mach 1.4 ¾ uncertainty Mach 1.4+		
		Heavy fuel	Mid fuel	Light fuel	Heavy fuel	Mid fuel	Light fuel
Roll limits	Min α	0	0	0	0	0	0
	Max α	6	18	19	0	0	0
	Min Nz	0	3	6	0	0	0
	Max Nz	6	18	19	0	0	0
	Max $\beta\bar{q}$	24	31	33	0	0	0
	ϕ	65	39	43	15	6	12
Roll HQ	ω_{dr}	0	40	38	0	0	0
	ζ_{dr}	0	40	38	0	0	0
Roll stability	GM	6	8	16	0	0	0
	PM	0	0	0	0	0	0
	BAS	16	32	37	0	0	0
Yaw limits	Min α	0	0	0	0	0	0
	Max α	6	21	29	0	0	0
	Min Nz	7	12	8	0	0	0
	Max Nz	12	29	36	0	0	0
	Max $\beta\bar{q}$	76	87	88	12	16	16
	ϕ	40	48	53	0	0	0
Yaw HQ	ω_{dr}	0	40	38	0	0	0
	ζ_{dr}	0	40	38	0	0	0
Yaw stability	GM	29	74	78	0	0	0
	PM	24	38	51	0	0	0
	BAS	16	32	37	0	0	0

Table 8. Test cases for piloted simulation evaluation.

Mach	Altitude (MSL)	Aero model	Boom position	Uncertainty aero	CAS	Axis	Fuel and uncertainty				Violations						
							Mid fuel full uncertainty	Mid fuel ¾ uncertainty	Light fuel full uncertainty	Light fuel ¾ uncertainty	Trim	Min Nz	Max Nz	$\beta\bar{q}$	ϕ	BAS	ζ_{sp}
0.95	18,000	DFRC	Extend	11	1	Pitch			X		X						
0.95	18,000	GS	Retract	9	0	Pitch	X					X					
0.95	18,000	GS	Retract	11	0	Pitch			X			X					
0.95	18,000	GS	Retract	2	0	Lat-dir	X					X		X	X		
0.95	18,000	GS	Retract	2	0	Lat-dir			X			X					
0.95	18,000	GS	Retract	6	0	Lat-dir	X						X		X		
0.95	18,000	GS	Retract	6	0	Lat-dir			X				X	X	X		
0.95	18,000	BL	Retract	2	0	Lat-dir			X			X					
0.95	18,000	BL	Retract	6	0	Lat-dir			X						X		
0.95	49,000	GS	Extend	10	1	Pitch	X				X						
0.95	18,000	GS	Extend	2	0	Lat-dir			X			X		X			
0.95	18,000	GS	Extend	2	0	Lat-dir	X					X		X	X		
0.95	49,000	GS	Retract	9	0	Lat-dir			X				X		X		X
0.95	18,000	GS	Extend	6	0	Lat-dir	X						X	X	X		
0.95	18,000	DTA	Extend	2	0	Lat-dir			X					X			
0.95	49,000	DFRC	Extend	1	0	Pitch			X							X	
0.95	49,000	GS	Extend	11	0	Pitch	X									X	
0.95	49,000	GS	Extend	12	0	Pitch	X										X
0.95	49,000	DTA	Extend	9	0	Pitch			X								X
0.95	49,000	DTA	Extend	9	0	Pitch	X									X	X
1.10	25,000	GS	Retract	5	0	Pitch	X					X					
1.10	25,000	GS	Retract	9	0	Pitch	X					X					
1.10	25,000	DTA	Extend	5	0	Pitch			X			X					
1.10	49,000	DTA	Extend	10	1	Pitch	X				X						
1.10	49,000	DTA	Extend	9	0	Pitch	X										X
1.20	45,000	BL	Retract	9	0	Pitch	X										X
1.40	45,000	DTA	Extend	9	0	Pitch	X										X
1.60	45,000	DTA	Extend	9	0	Pitch		X									X
1.80	45,000	BL	Retract	9	0	Pitch		X									X
1.40	40,000	GS	Retract	6	0	Lat-dir	X							X			
1.40	40,000	GS	Extend	6	0	Lat-dir	X							X			
1.80	45,000	DTA	Extend	6	0	Lat-dir		X						X			
1.80	45,000	GS	Retract	9	0	Pitch				X		X					
1.80	45,000	DTA	Retract	9	0	Pitch				X							X
1.80	45,000	GS	Retract	6	0	Lat-dir				X				X			

FIGURES

ED06-0184

Figure 1. NASA F-15B modified with Gulfstream Aerospace Corporation Quiet Spike™ shown in the fully extended position.

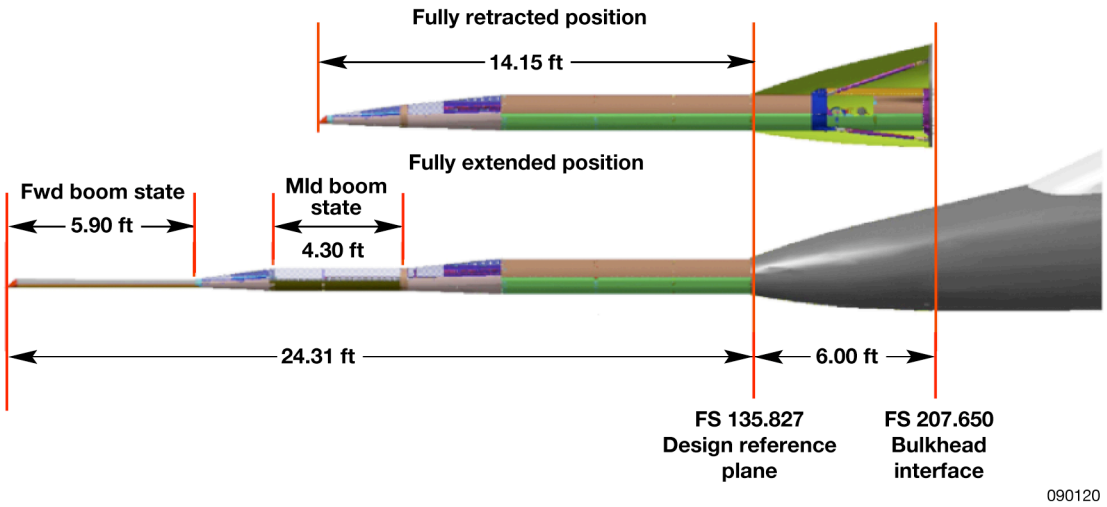

Figure 2. The Quiet Spike™ configuration.

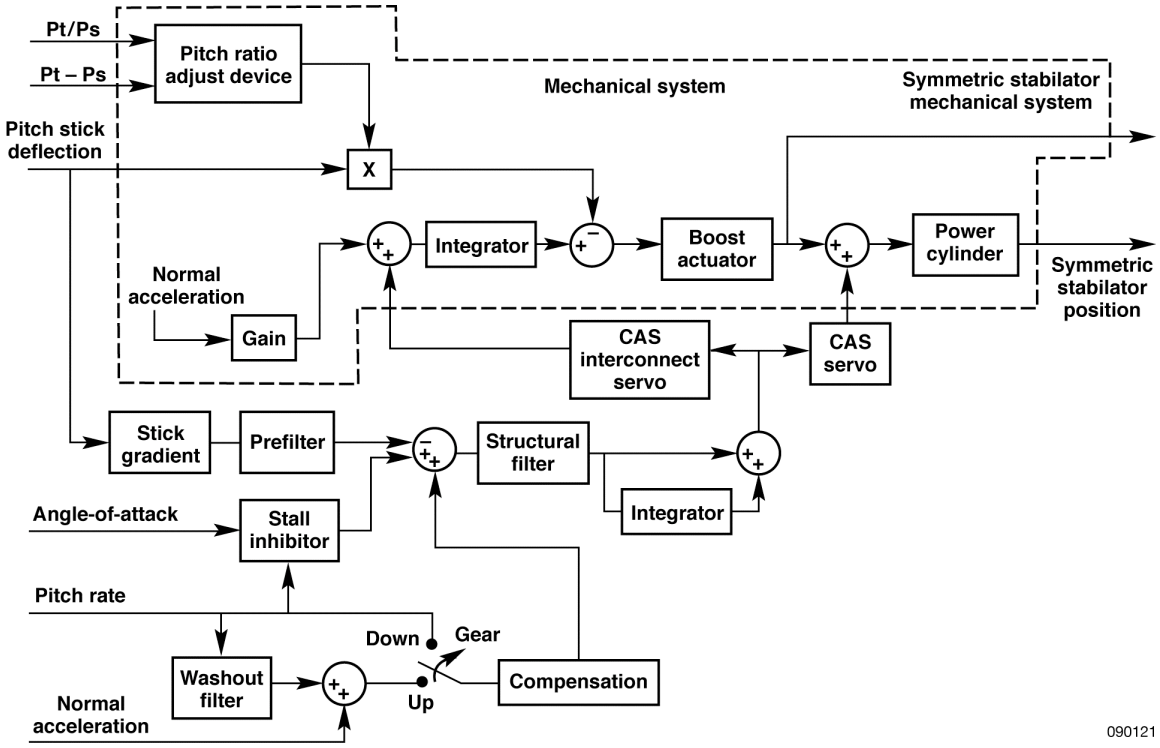

Figure 3. A simplified pitch axis control model for the NASA DFRC F-15B.

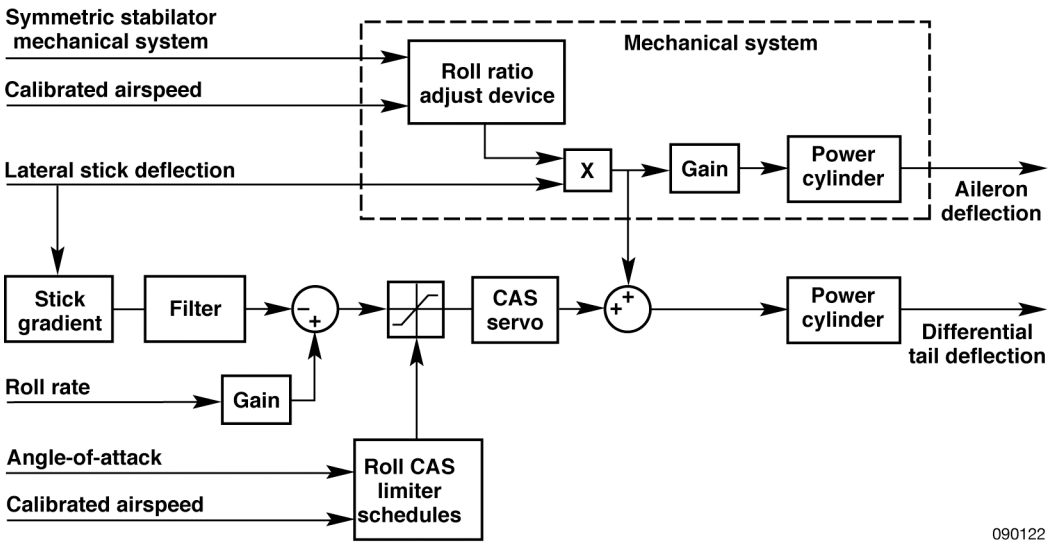

Figure 4. A simplified roll axis control model for the NASA DFRC F-15B.

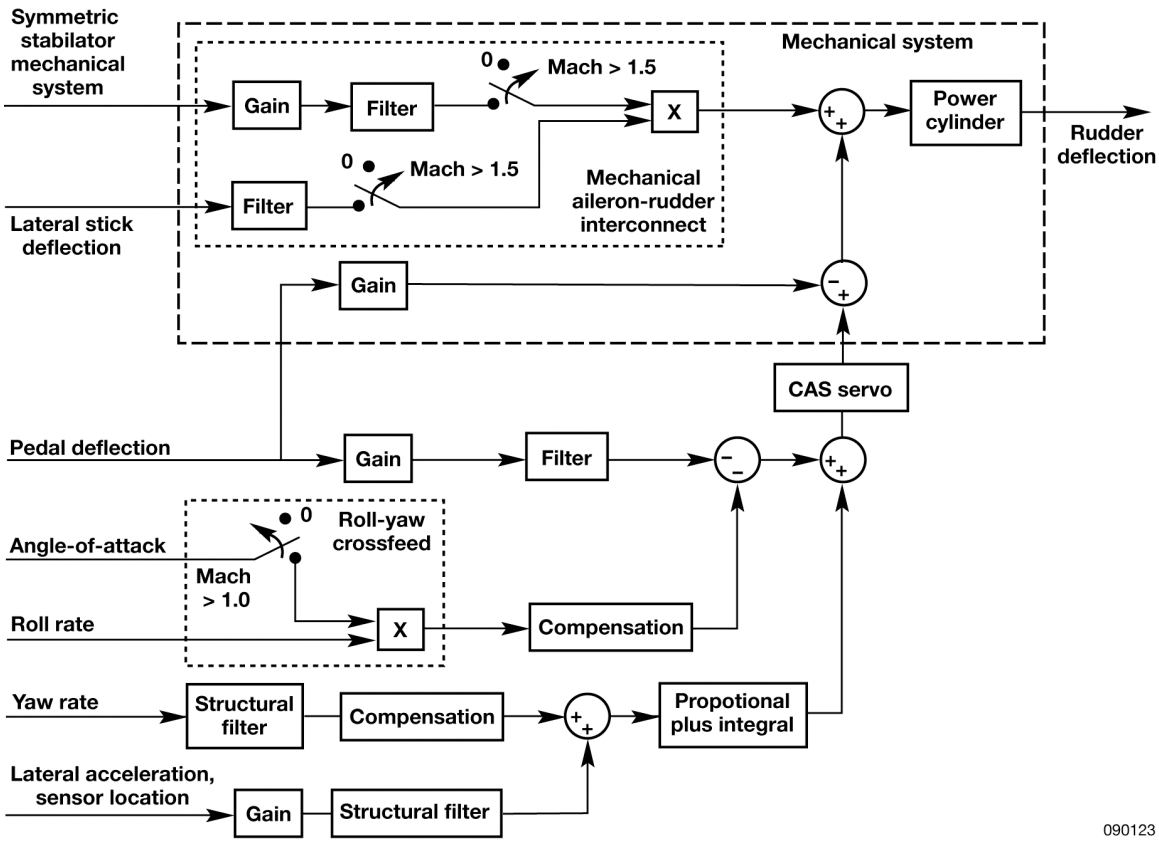

Figure 5. A simplified yaw axis control model for the NASA DFRC F-15B.

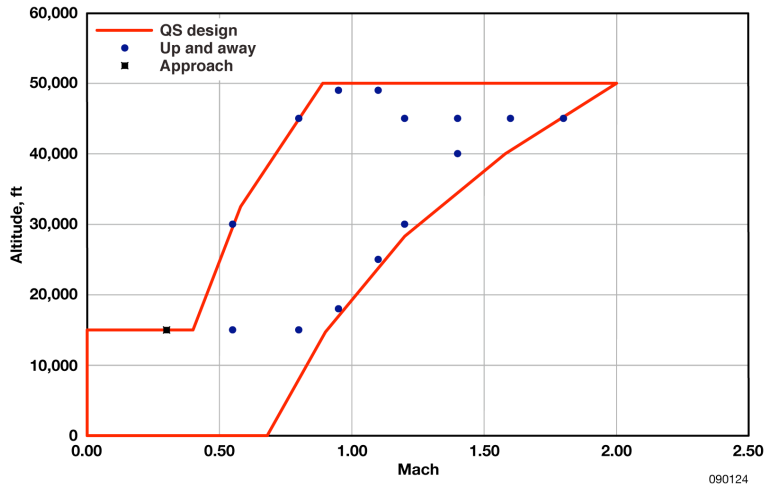

Figure 6. Quiet Spike™ flight test envelope and conditions at which analysis was performed.

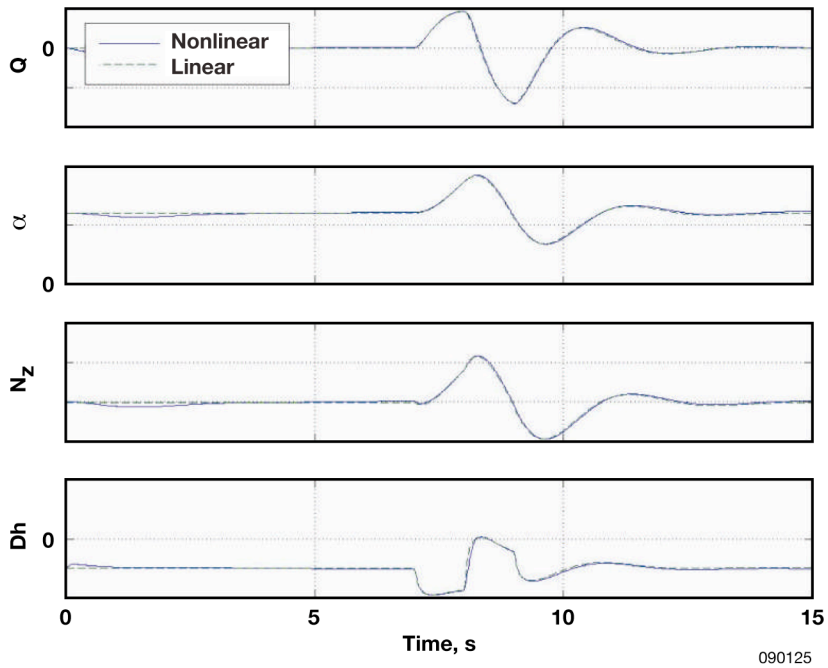

Figure 7. CAS on time history responses of the nominal airplane from a pitch doublet at an altitude of 45,000 ft, at Mach 0.8.

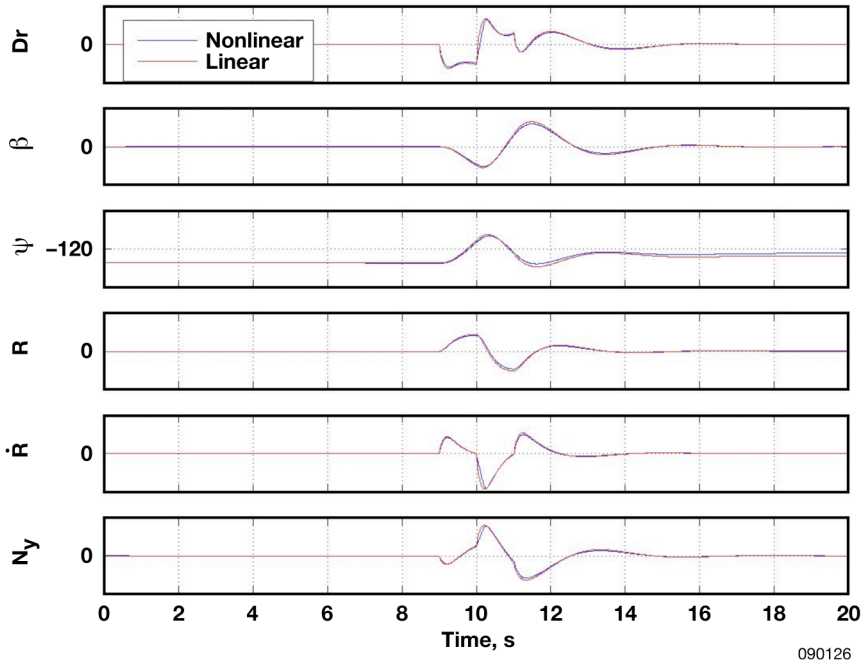

Figure 8. CAS on time history responses of the nominal airplane from a yaw doublet at an altitude of 45,000 ft, at Mach 0.8.

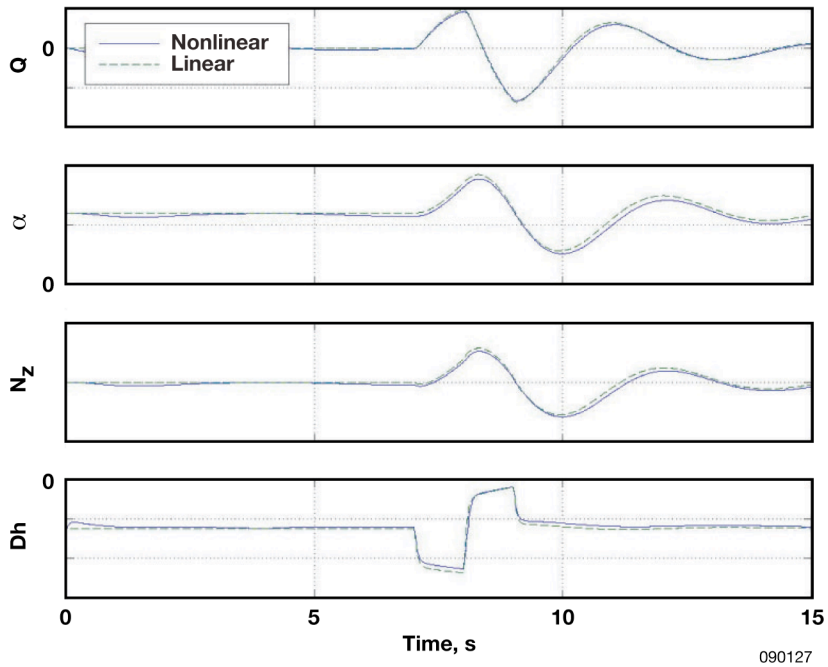

Figure 9. CAS off time history responses of the nominal airplane from a pitch doublet at an altitude of 45,000 ft, at Mach 0.8.

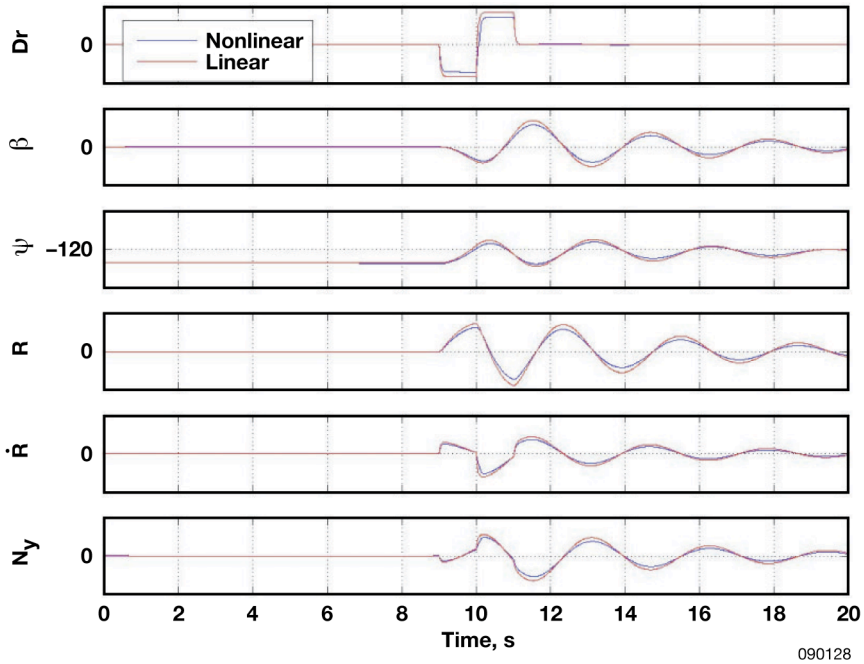

Figure 10. CAS off time history responses of the nominal airplane from a yaw doublet at an altitude of 45,000 ft, at Mach 0.8.

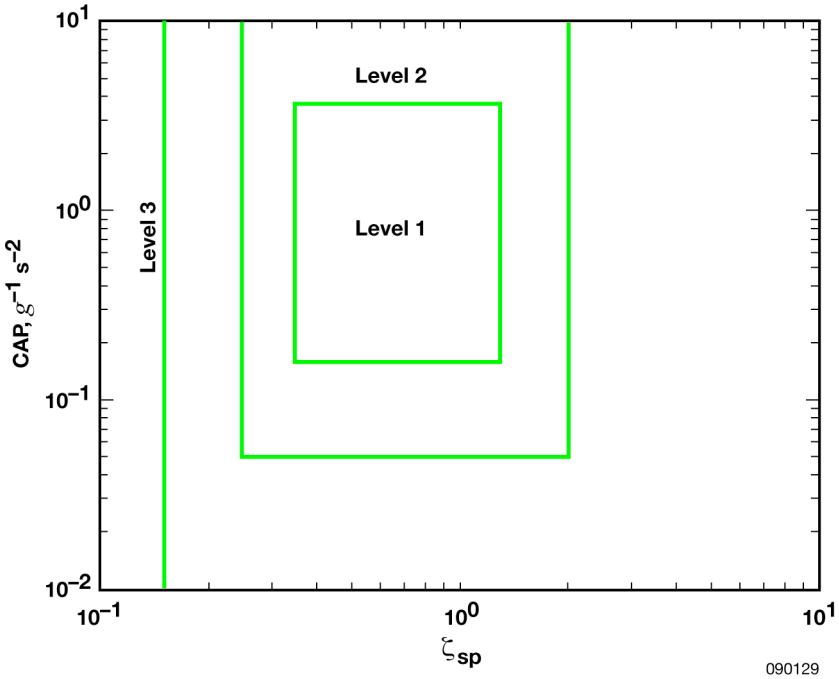

Figure 11. Handling qualities metrics definition.

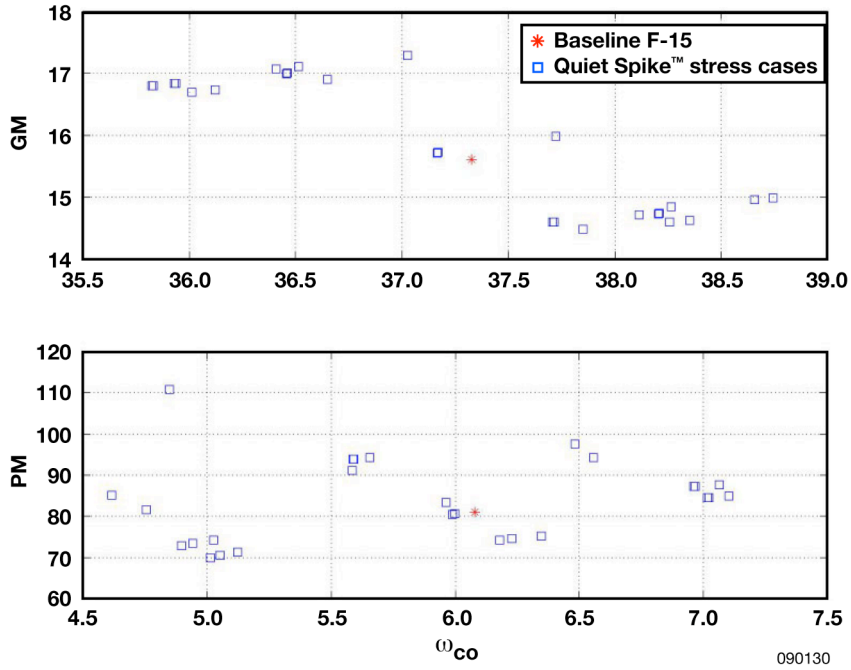

Figure 12. Stability margin family plot at an altitude of 15,000 ft, at Mach 0.8, with fuel weight of 8,000 lb, and CAS on.

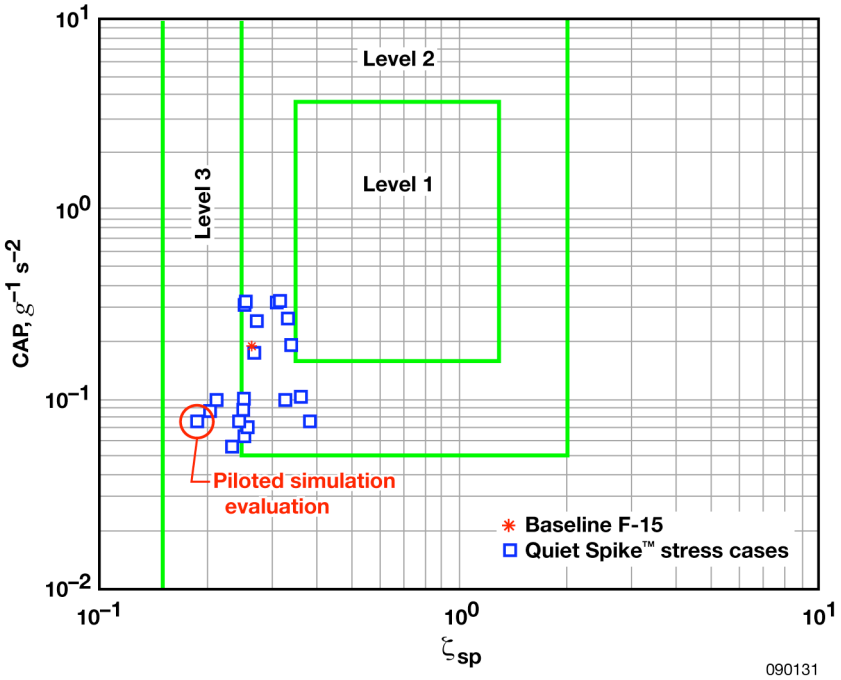

Figure 13. Pitch axis handling qualities at an altitude of 45,000 ft, at Mach 0.8, with fuel weight of 2,000 lb, and CAS off.

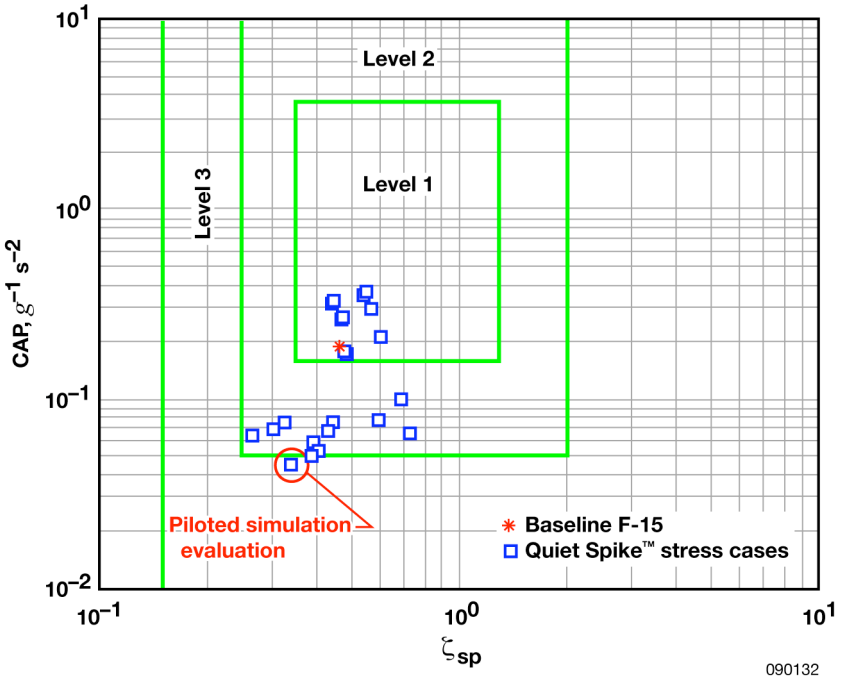

Figure 14. Pitch axis handling qualities at an altitude of 15,000 ft, at Mach 0.8, with fuel weight of 2,000 lb, and CAS off.

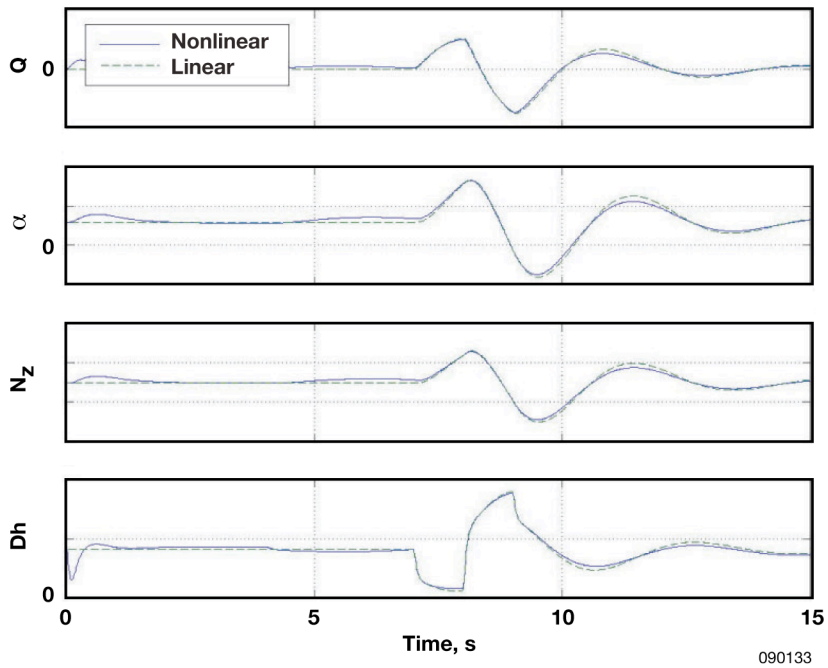

Figure 15. CAS off time history responses at an altitude of 15,000 ft, at Mach 0.8, with the Gulfstream spike model, with fuel weight of 2,000 lb, and stress case 9.

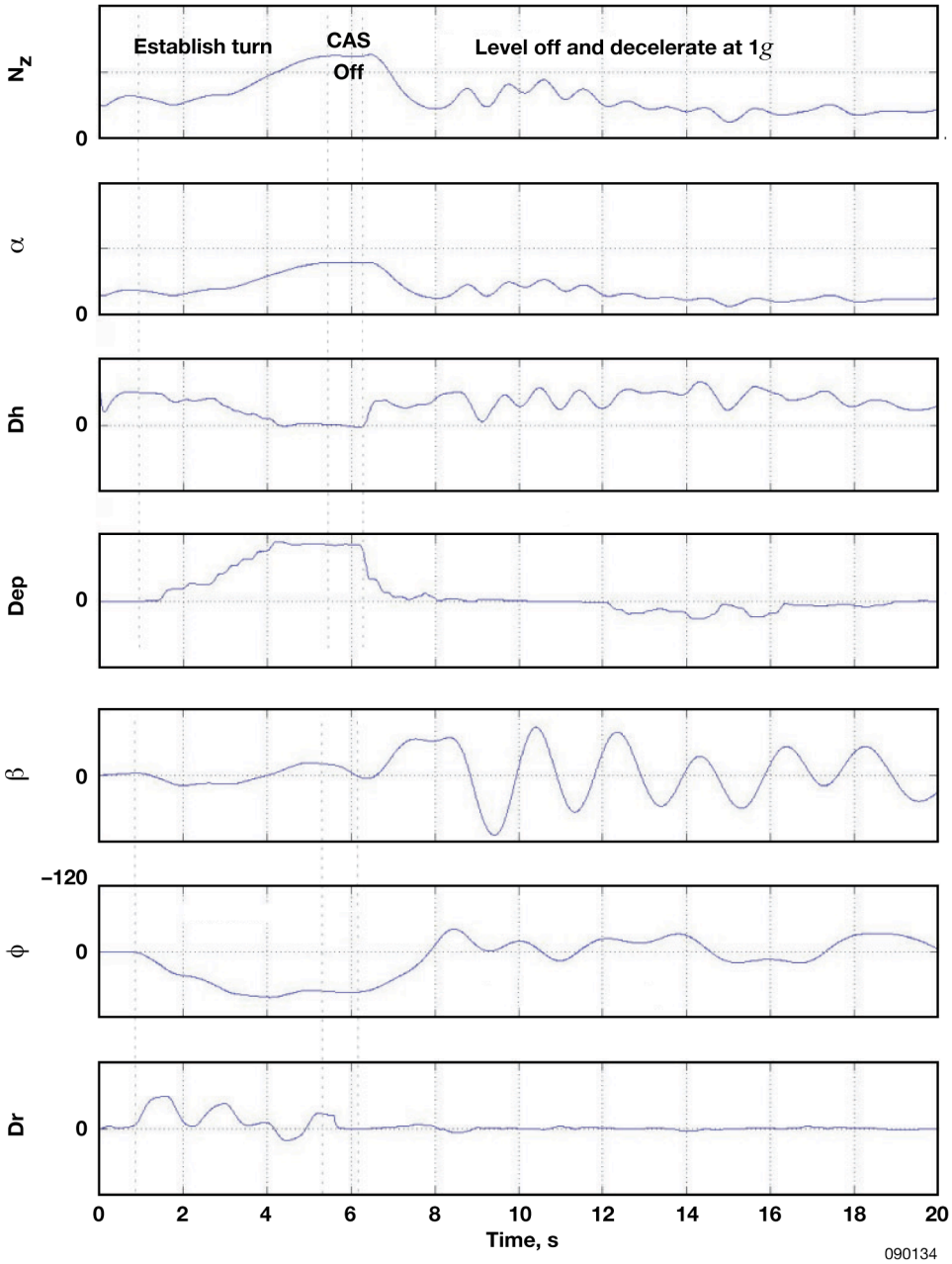

Figure 16. Time history of pilot evaluation at an altitude of 15,000 ft, at Mach 0.8 with the Gulfstream spike model, with fuel weight of 8,000 lb, and stress case 2.

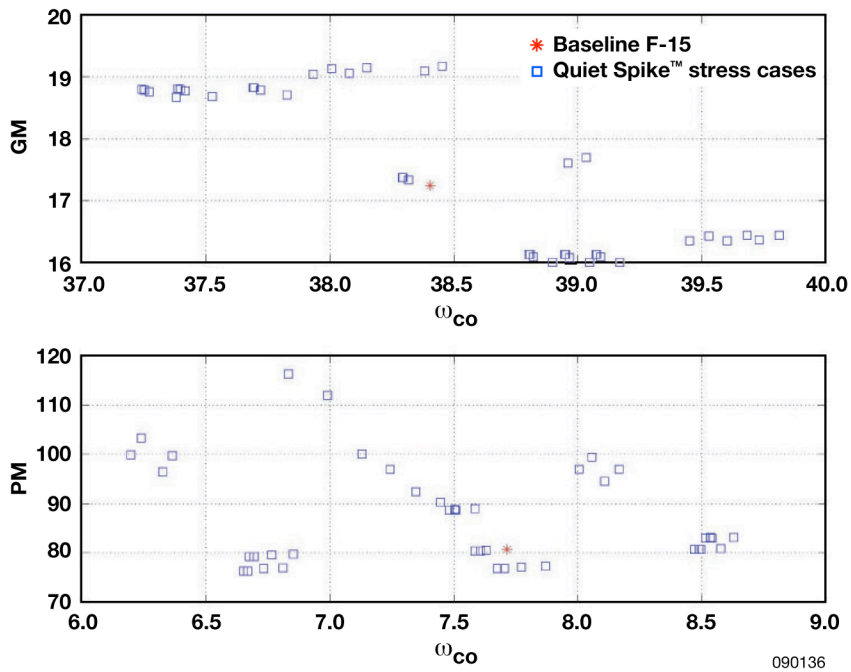

Figure 17. Gain and phase margin for flight condition at an altitude of 45,000 ft, at Mach 1.8, and CAS on.

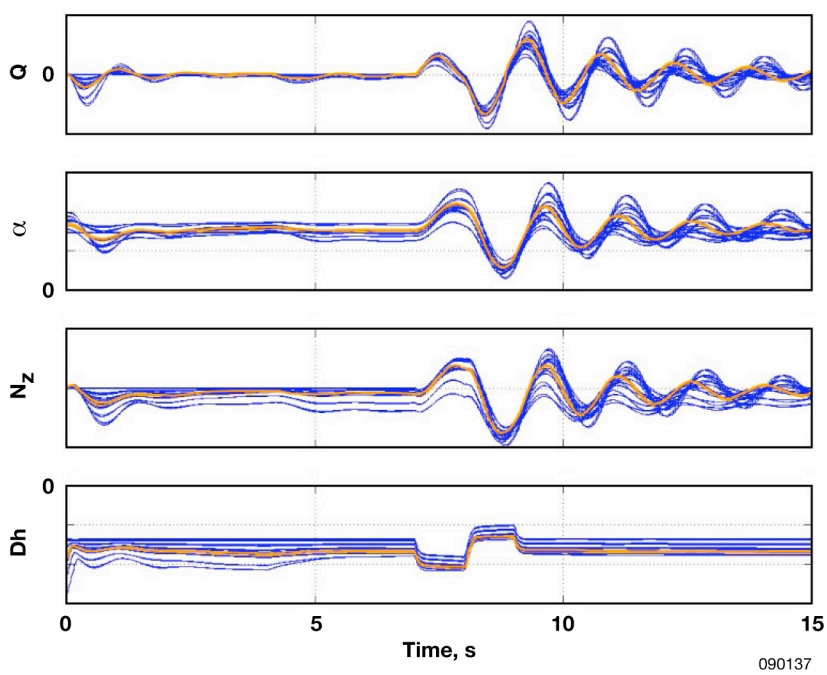

Figure 18. Family curve time history plots showing low damping at an altitude of 49,000 ft, at Mach 1.1, and CAS off.

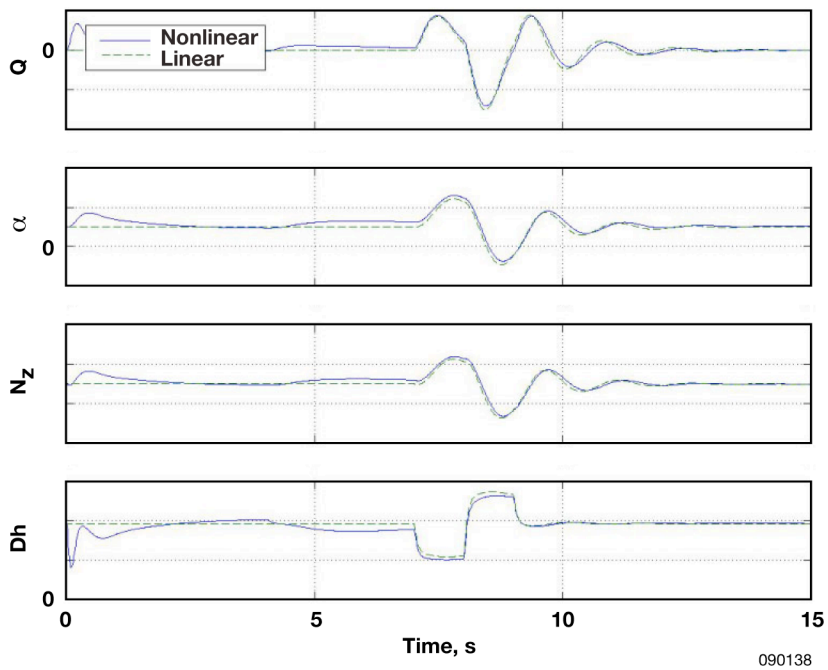

Figure 19. Nz excursion for low fuel weight at an altitude of 18,000 ft, at Mach 0.95, with Gulf Stream spike retracted, CAS off, and stress case 9.

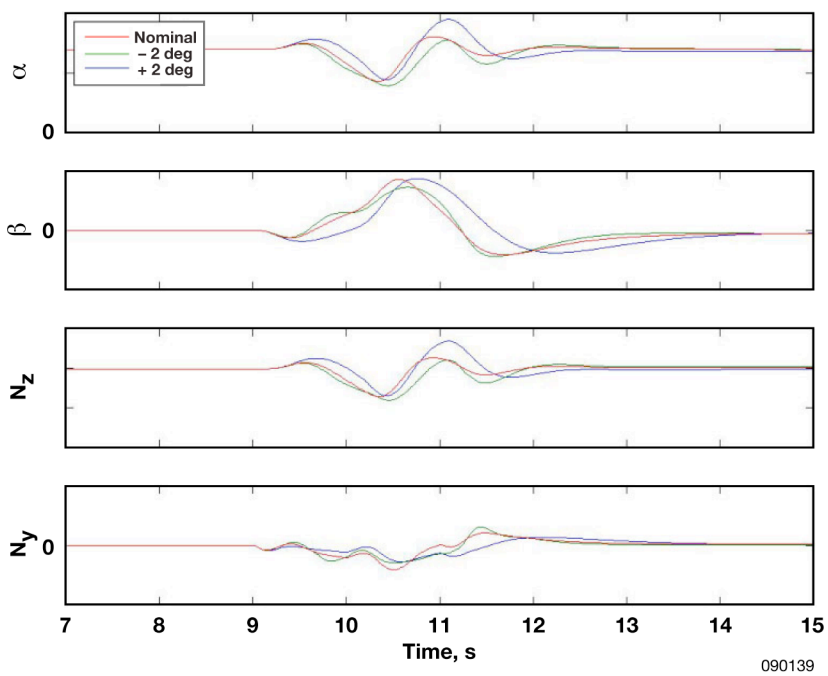

Figure 20. Time histories for a 2-inch lateral doublet with pitch CAS on, at an altitude of 15,000 ft, at Mach 0.8.

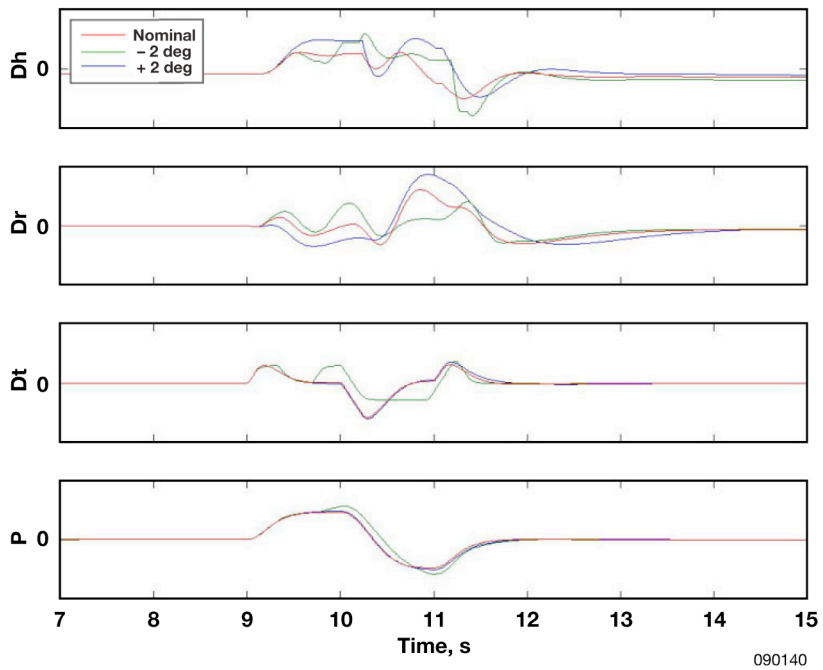

Figure 21. Time histories for a 2-inch lateral doublet with pitch CAS on, at an altitude of 15,000 ft, at Mach 0.8.

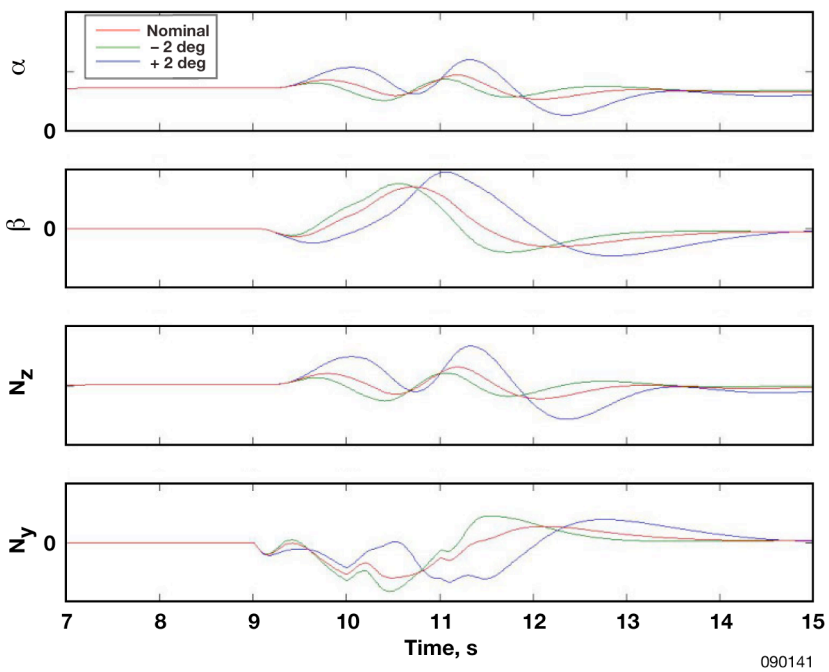

Figure 22. Time histories for a 2-inch lateral doublet with pitch CAS off, at an altitude of 15,000 ft, at Mach 0.8.

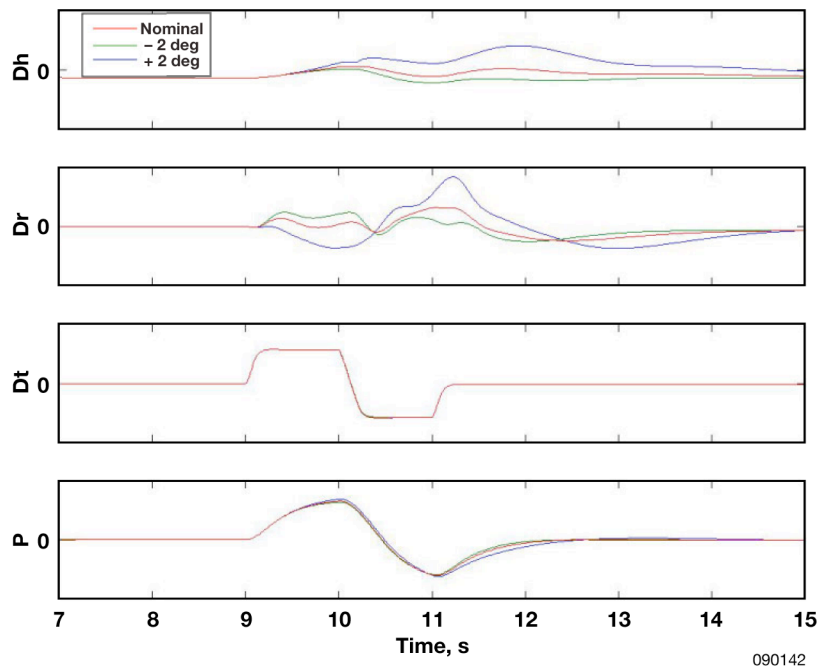

Figure 23. Time histories for a 2-inch lateral doublet with pitch CAS off, at an altitude of 15,000 ft, at Mach 0.8.

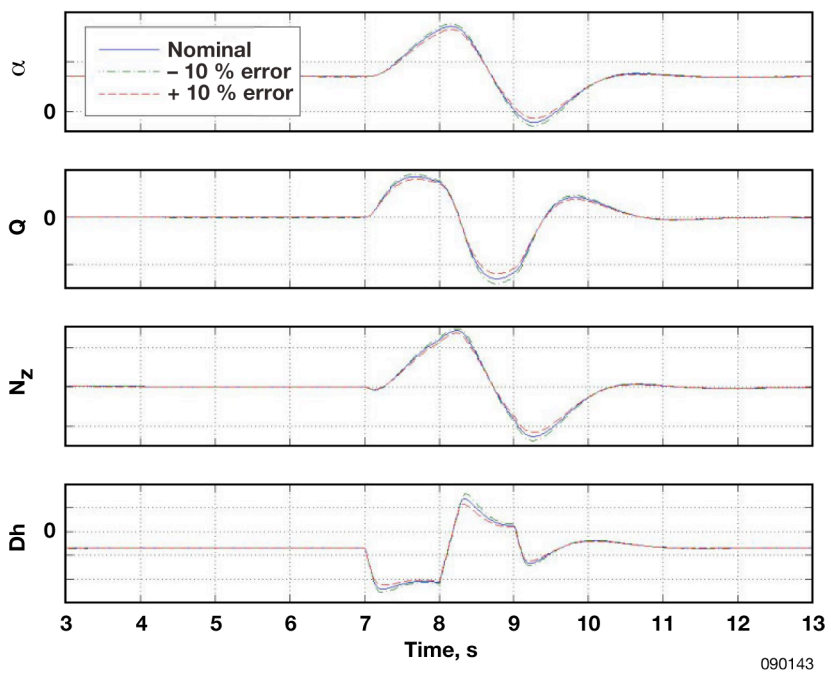

Figure 24. Time history comparisons of the nominal simulation response with responses that include +/ - 10% error in air data.

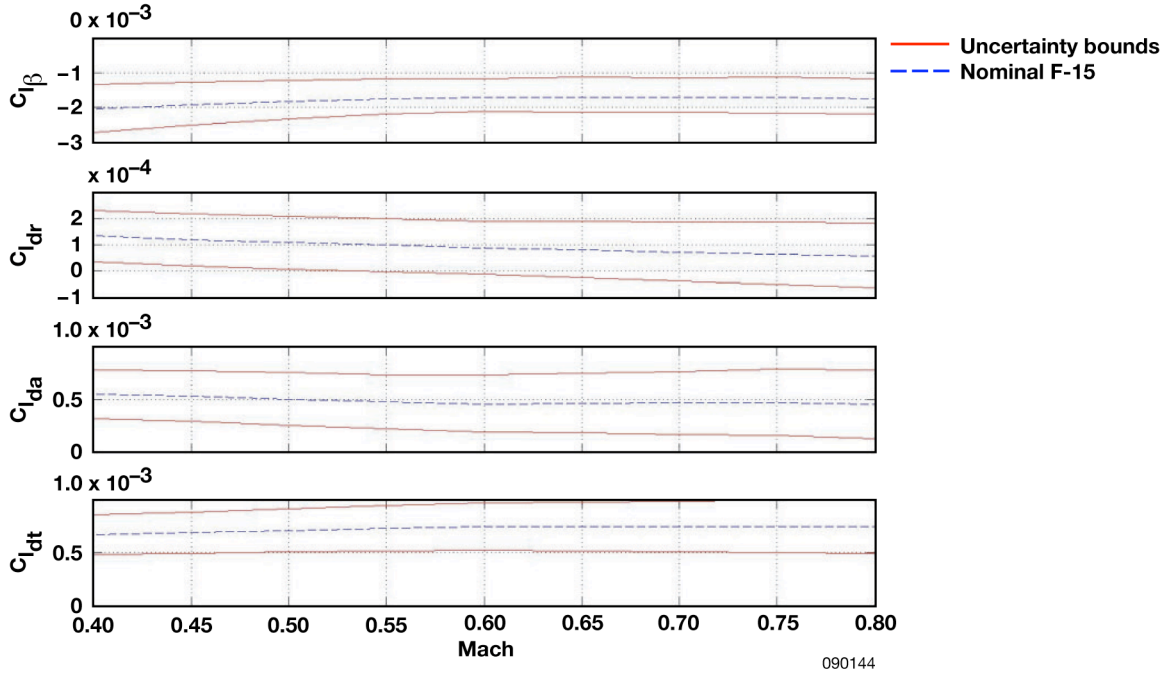

Figure 25. Rolling moment parameter variation up to Mach 0.8.

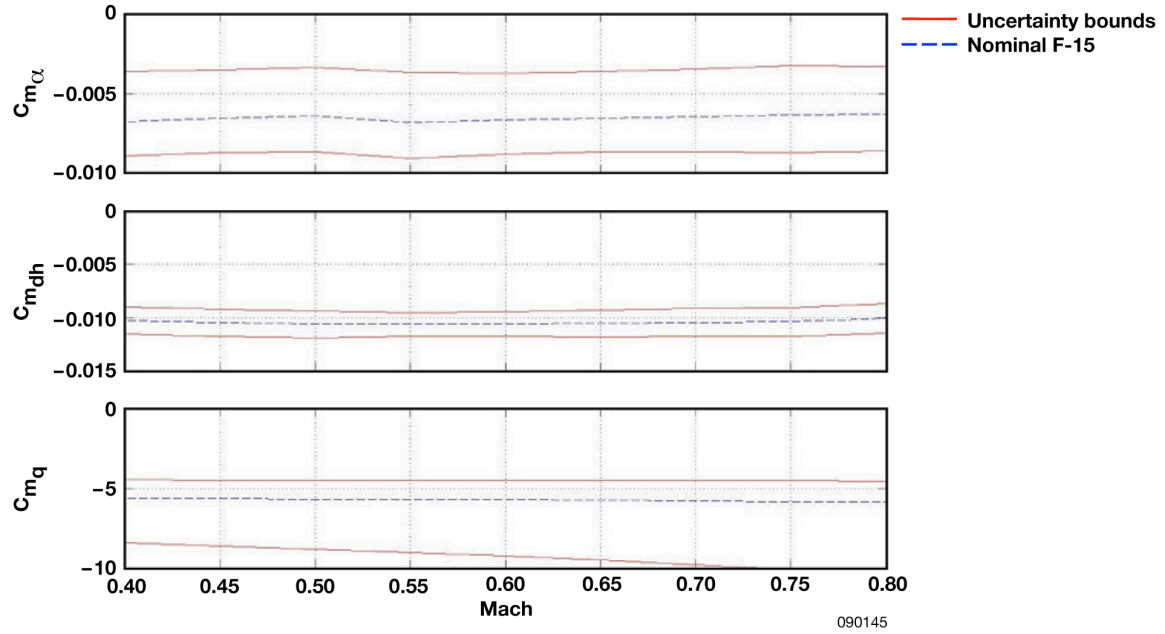

Figure 26. Pitch moment parameter variations up to Mach 0.8.

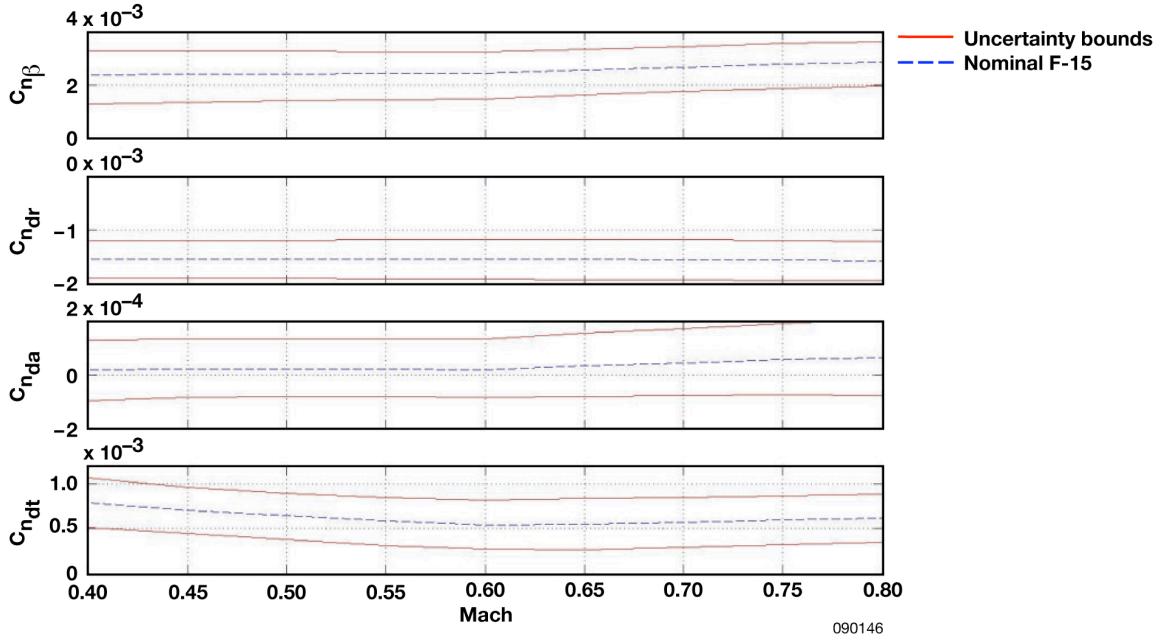

Figure 27. Yawing moment parameter variations up to Mach 0.8.

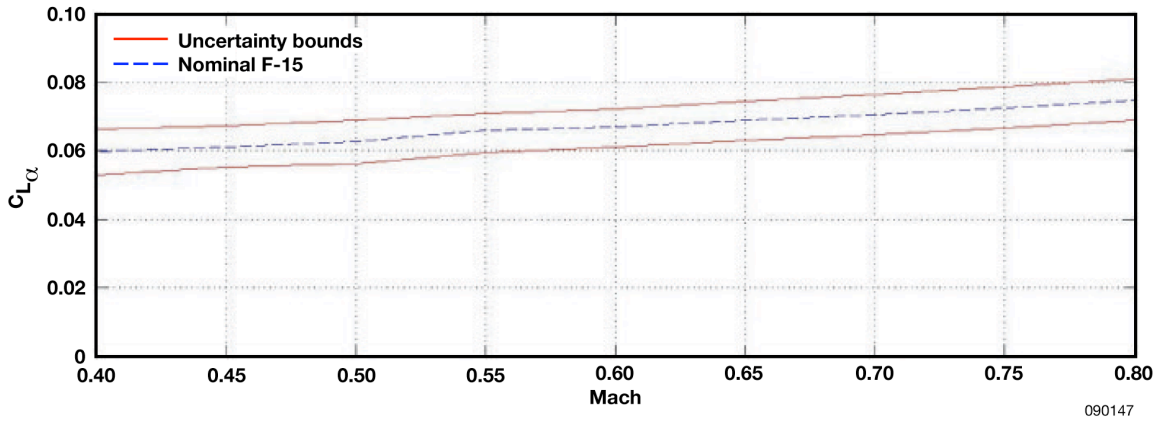

Figure 28. Lift force C_{L_α} due to angle-of-attack.

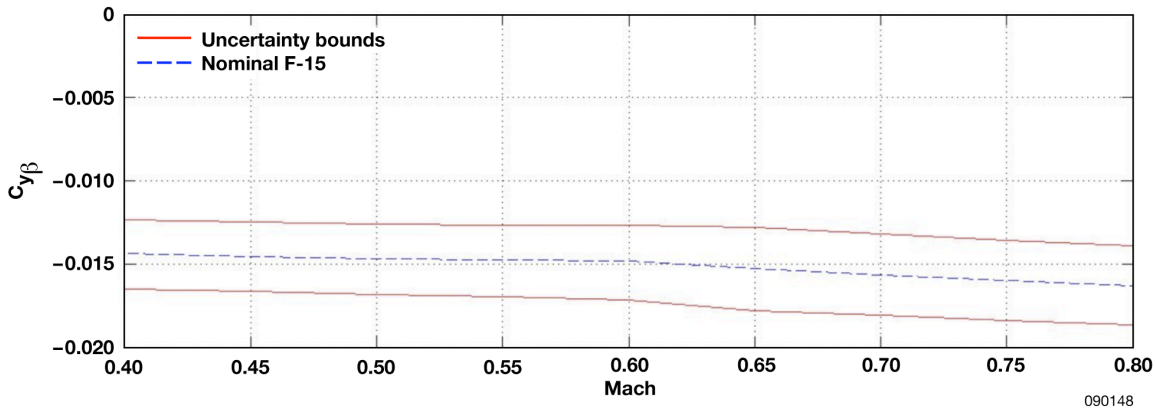

Figure 29 Side force C_{y_β} due to sideslip.

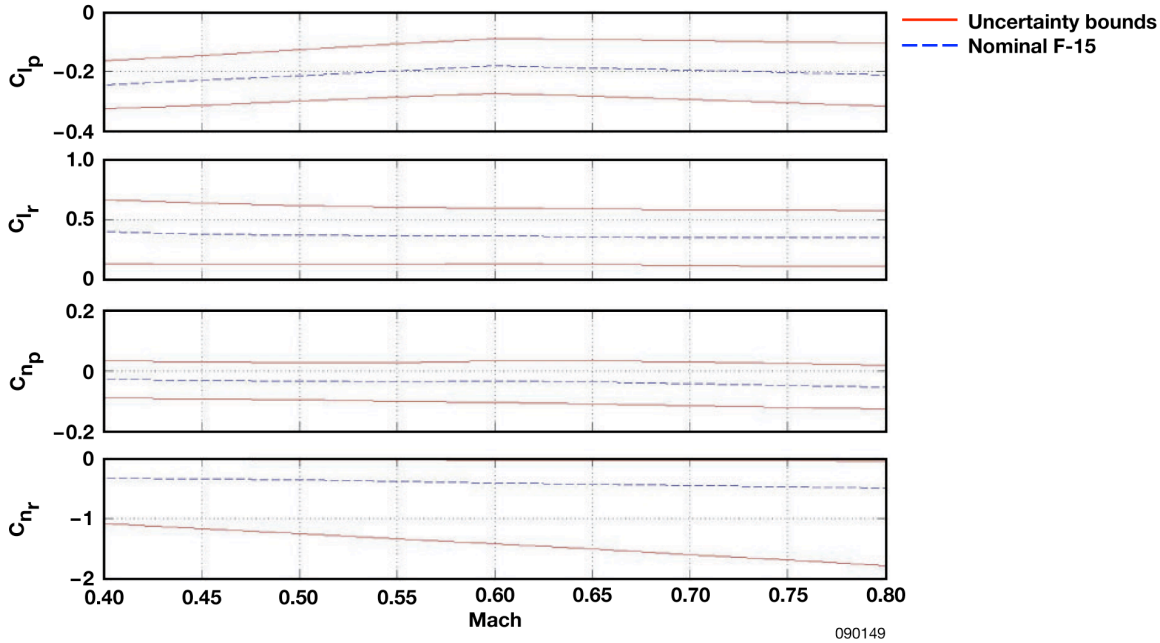

Figure 30. Damping derivatives up to Mach 0.8.

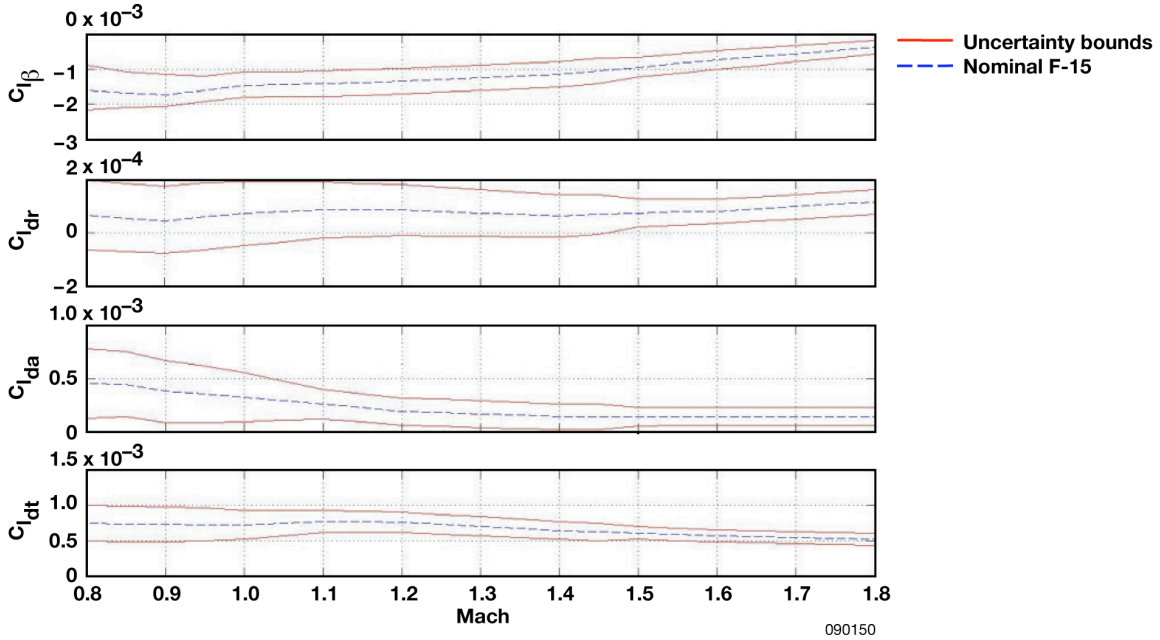

Figure 31. Rolling moment parameter variations from Mach 0.8 to Mach 1.8.

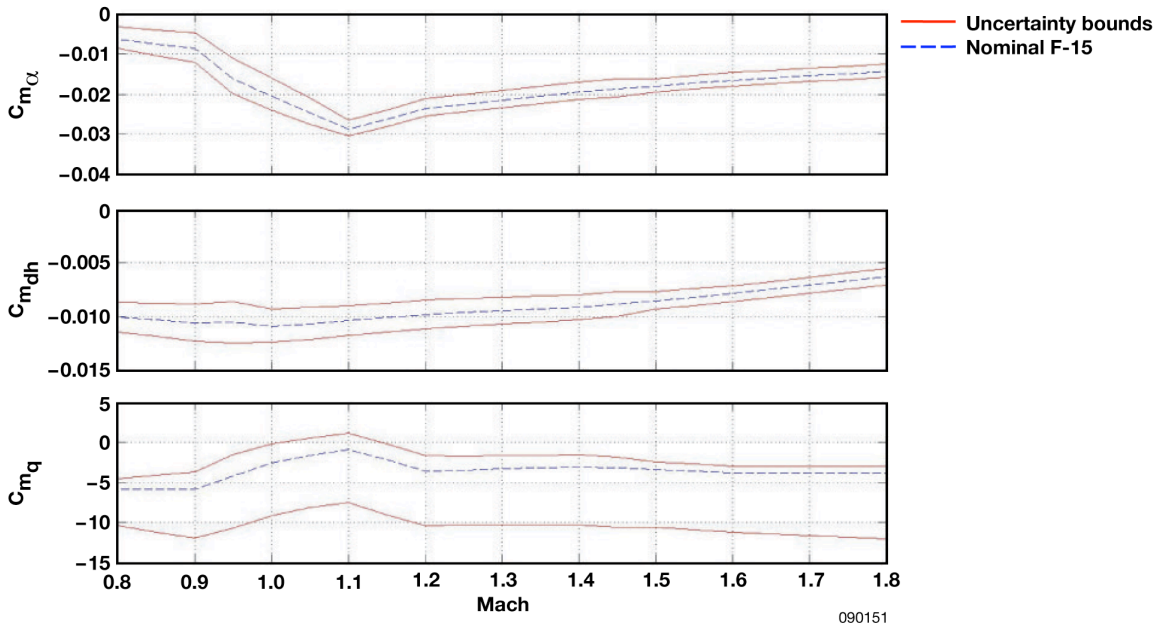

Figure 32. Pitch moment parameter variations from Mach 0.8 to Mach 1.8.

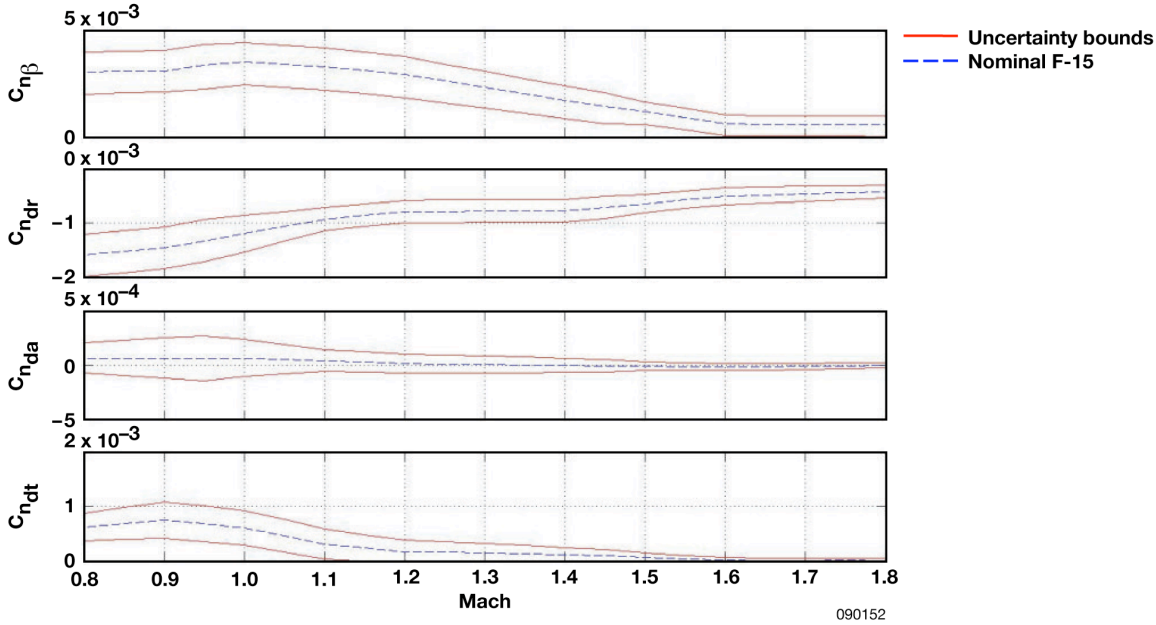

Figure 33. Yawing moment parameter variations from Mach 0.8 to Mach 1.8.

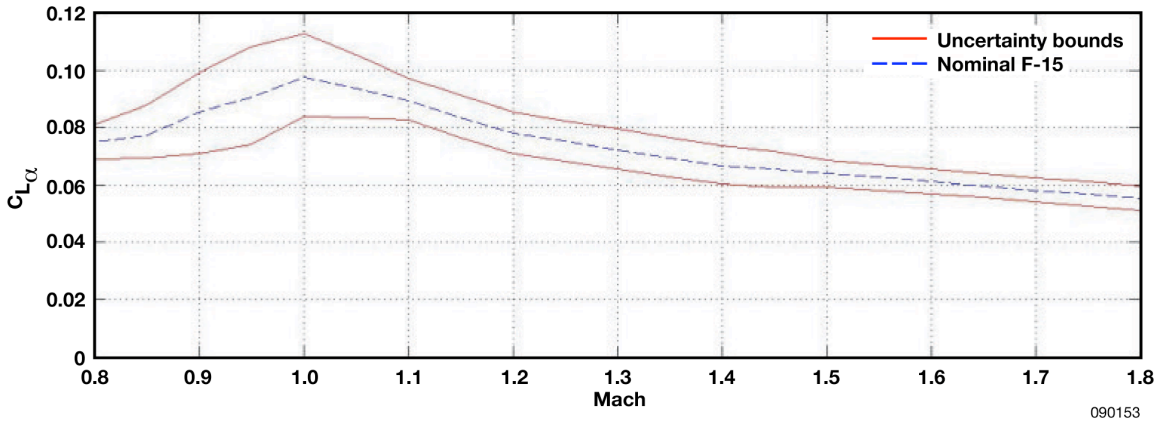

Figure 34. Lift force C_{L_α} due to angle-of-attack from Mach 0.8 to Mach 1.8.

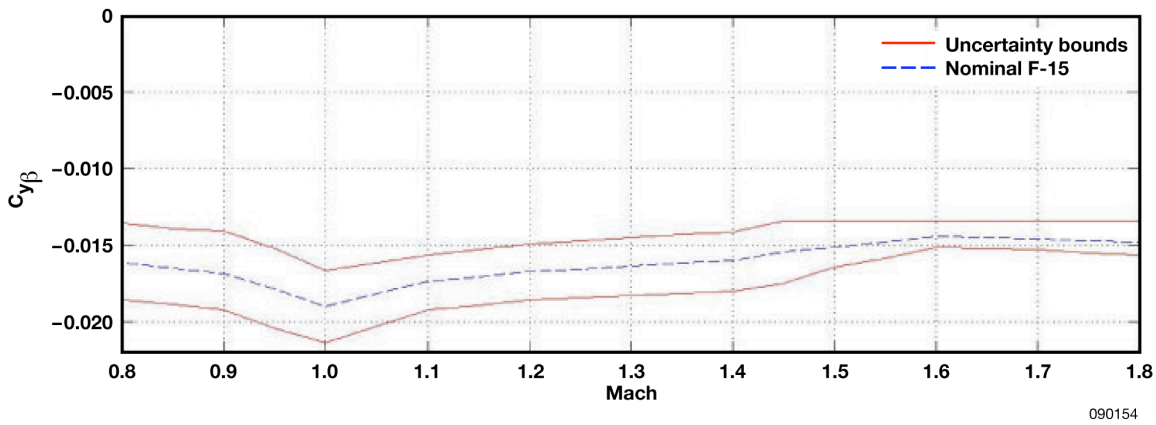

Figure 35. Side force C_{y_β} due to sideslip from Mach 0.8 to Mach 1.8.

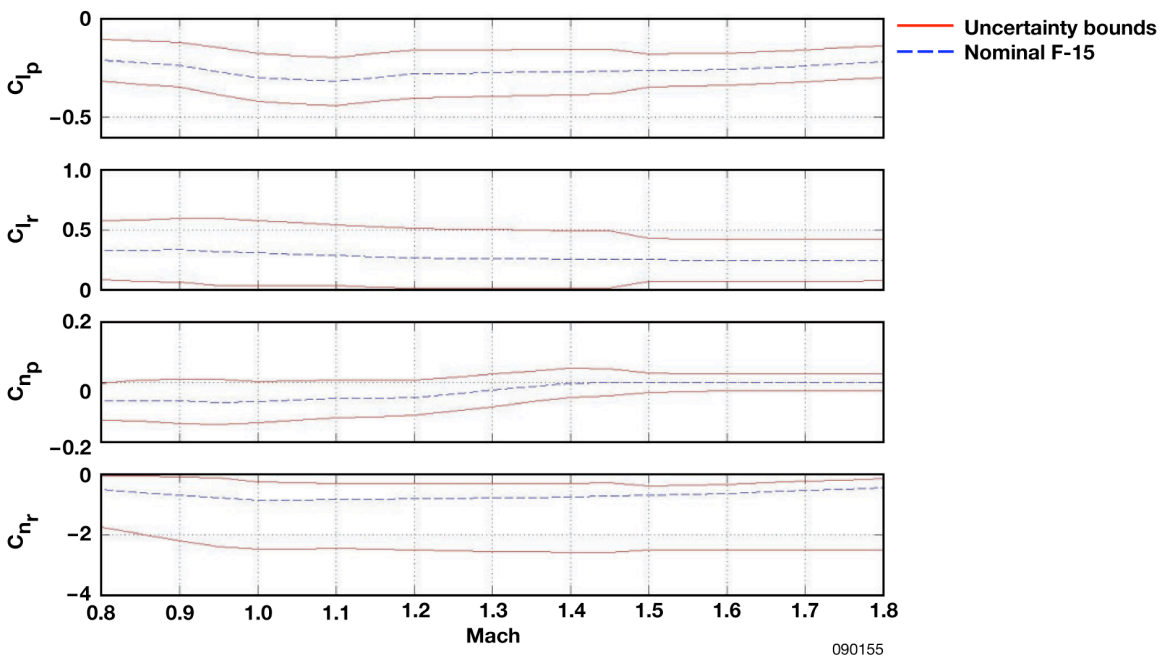

Figure 36. Damping derivatives from Mach 0.8 to Mach 1.8.

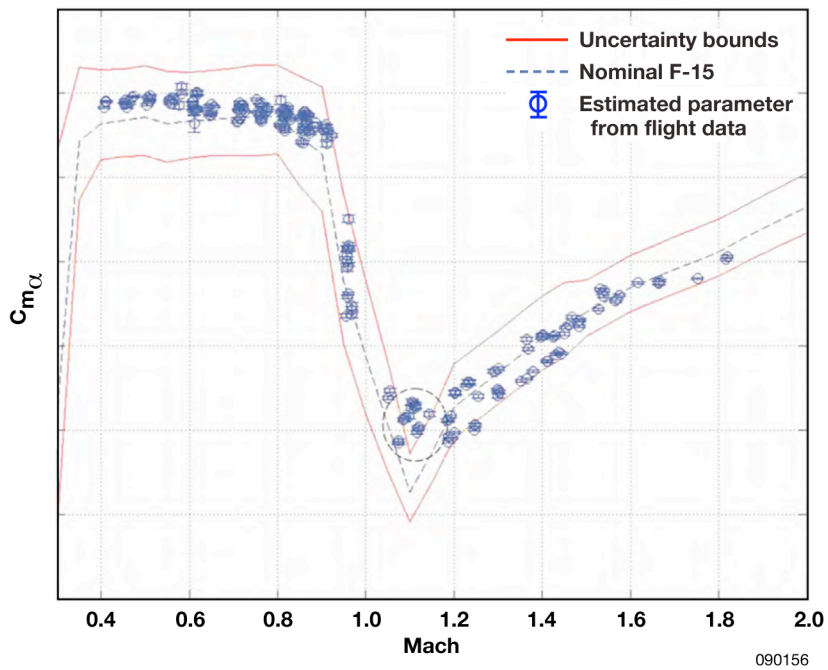

Figure 37. Stability and control derivative, C_{m_α} .

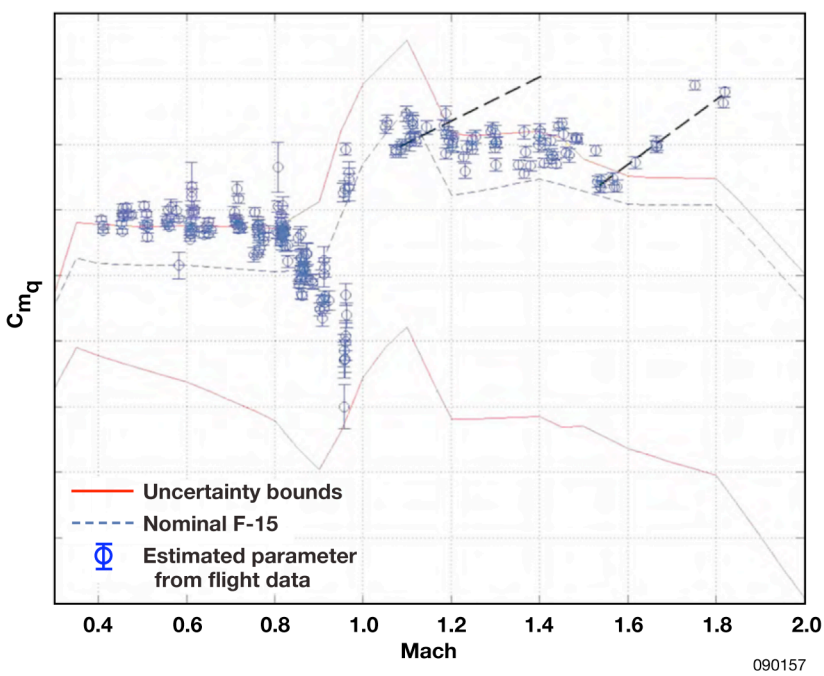

Figure 38. Stability and control derivative, C_{m_q} .

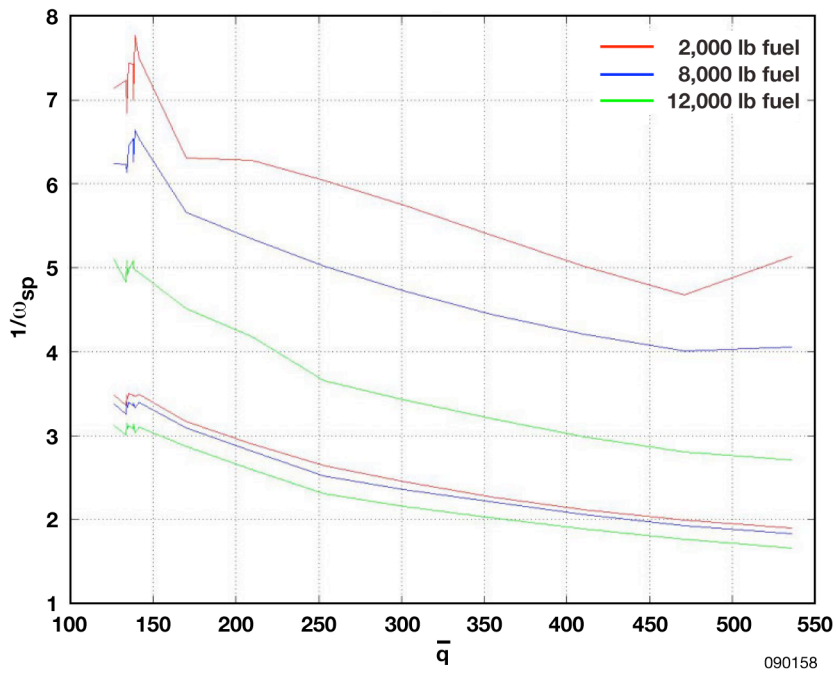

Figure 39. Short period mode for subsonic, CAS off clearance envelopes.

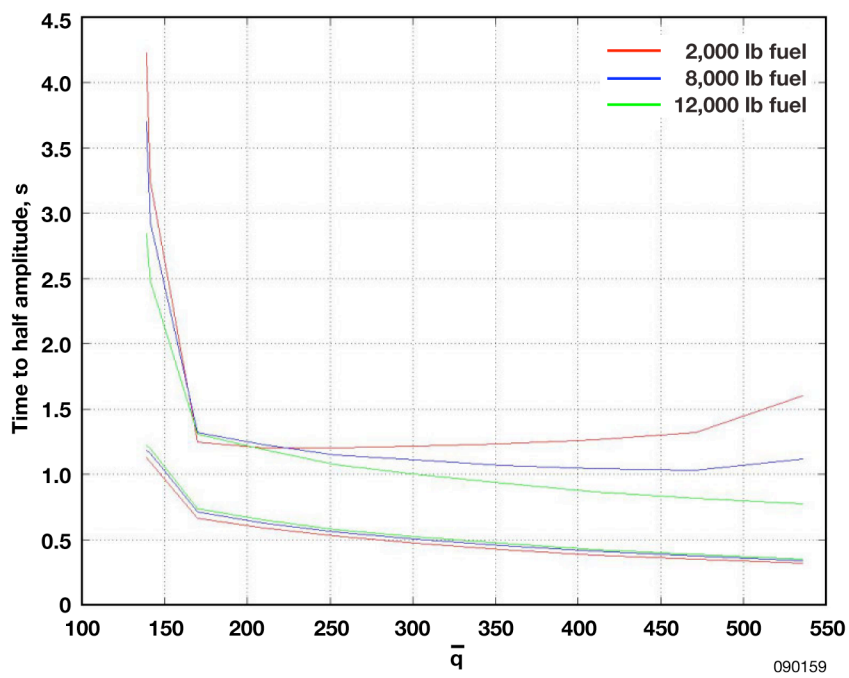

Figure 40. Time-to-half of the short period mode for subsonic, CAS off clearance envelopes.

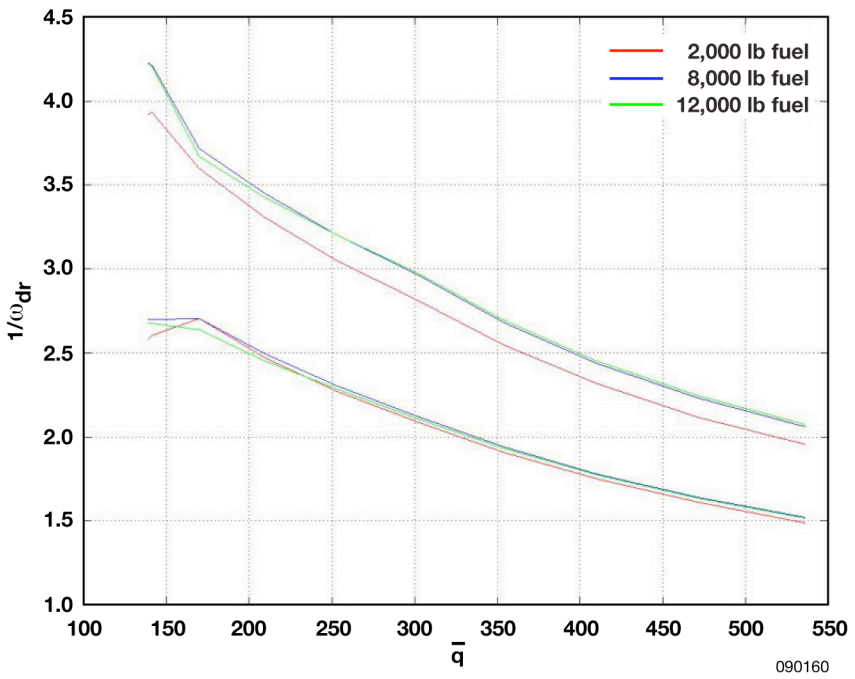

Figure 41. Period of the Dutch roll mode for subsonic, CAS off clearance envelopes.

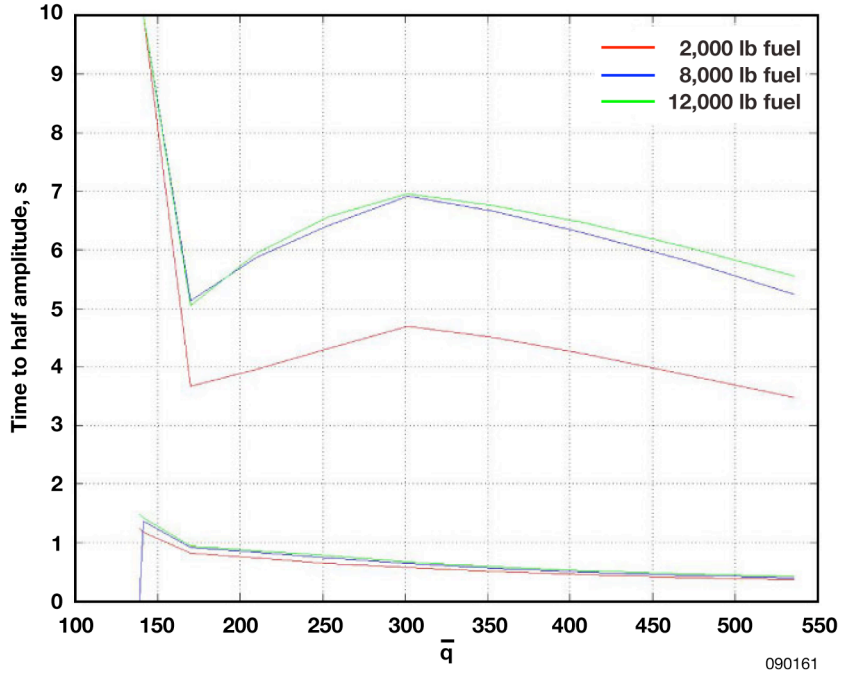

Figure 42. Time-to-half of the Dutch roll mode for subsonic, CAS off clearance envelopes.

REFERENCES

1. Henne, Preston A., "Case for Small Supersonic Civil Aircraft," AIAA Journal of Aircraft, Vol. 42, No. 3, pp. 765-774, May-June 2005.

2. Wolz, R., "A Summary of Recent Supersonic Vehicle Studies at Gulfstream Aerospace," AIAA-2003-0558, *Proceedings of the 41st AIAA Aerospace Sciences Meeting and Exhibit*, Reno, Nevada, January 6-9, 2003.

3. Howe, Donald C., "Sonic Boom Reduction Through the Use of Non-Axsymmetric Configuration Shaping," AIAA-2003-0929, *Proceedings of the 41st AIAA Aerospace Sciences Meeting and Exhibit*, Reno, Nevada, January 6-9, 2003.

4. Henne, Preston A., Donald C. Howe, Robert R. Wolz, and Jimmy L. Hancock Jr., *Supersonic Aircraft with Spike for Controlling and Reducing Sonic Boom*, U.S. Patent Number 6,698,684 B1, issued March 2, 2004.

5. Howe, Donald C., "Improved Sonic Boom Minimization with Extendable Nose Spike," AIAA-2005-1014, *Proceedings of the 43rd AIAA Aerospace Sciences Meeting and Exhibit*, Reno, Nevada, January 10-13, 2005.

6. Simmons, Frank, and Donald Freund, "Morphing Concept for Quiet Supersonic Jet Boom Mitigation," AIAA-2005-1015, *Proceedings of the 43rd AIAA Aerospace Sciences Meeting and Exhibit*, Reno, Nevada, January 10-13, 2005.

7. Simmons III, Frank, Donald Freund, Natalie D. Spivey, and Lawrence Schuster, "Quiet Spike™: The Design and Validation of an Extendable Nose Boom Prototype," AIAA-2007-1774, *Proceedings of the 48th AIAA/ASME/ASCE/AHS/ASC Structures, Structural Dynamics, and Materials Conference,* Honolulu, Hawaii, April 23-26, 2007.

8. Spivey, Natalie, Claudia Y. Herrera, Roger Truax, Chan-gi Pak, and Donald Freund, "Quiet Spike™ Build-up Ground Vibration Testing Approach," AIAA-2007-1175, Proceedings of the 48th *AIAA/ASME/ASCE/AHS/ASC Structures, Structural Dynamics, and Materials Conference*, Honolulu, Hawaii, April 23-26, 2007.

9. Herrera, Claudia. Y., and Chan-gi Pak, "Build-up Approach to Updating the Mock Quiet Spike™ Beam Model," AIAA-2007-1776, *Proceedings of the 48th AIAA/ASME/ASCE/AHS/ASC Structures, Structural Dynamics, and Materials Conference*, Honolulu, Hawaii, April 23-26, 2007.

10. Haering Jr., Edward A., James E. Murray, Dana D. Purifoy, David H. Graham, Keith B. Meredith, Christopher E. Ashburn, and Lt. Col. Mark Stucky, "Airborne Shaped Sonic Boom Demonstration Pressure Measurements with Computational Fluid Dynamics Comparisons," AIAA-2005-0009, *Proceedings of the 43rd AIAA Aerospace Sciences Meeting and Exhibit*, Reno, Nevada, January 10-13, 2005.

11. Smolka, James W., Robert A. Cowart, Leslie M. Molzahn, Thomas J. Grindle, Tim Cox, and Steve Cumming et al., "Flight Testing of the Gulfstream Quiet Spike™ on a NASA F-15B," *Proceedings of the Society of Experimental Test Pilots 51st Symposium and Banquet*, Anaheim, California, September 26-29, 2007.

12. Cumming, Stephen B., Mark S. Smith, and Michael A. Frederick, "Aerodynamic Effects of a 24-Foot, Multisegmented Telescoping Nose Boom on an F- 15B," AIAA-2007-6638, *Proceedings of the AIAA Atmospheric Flight Mechanics Conference and Exhibit*, Hilton Head, South Carolina, August 20-23, 2007.

13. Moua, Cheng M., Shaun C. McWherter, Timothy H. Cox, and Joseph Gera, *Flight Test Results on the Stability and Control of the F-15B Quiet Spike™ Aircraft*, "not yet published."

14. Freund, Donald, Frank Simmons III, Natalie D. Spivey, and Lawrence Schuster, "Quiet Spike™ Prototype Flight Test Results," AIAA-2007-1778, *Proceedings of the 48th AIAA/ASME/ASCE/AHS/ASC Structures, Structural Dynamics, and Materials Conference*, Honolulu, Hawaii, April 23-26, 2007.

15. Norlin, Ken A., *Flight Simulation Software at NASA Dryden Flight Research Center*, NASA TM-104315, 1995.

16. Flying Qualities of Piloted Vehicles, MIL-STD-1797, March 31, 1987.

REPORT DOCUMENTATION PAGE

Form Approved
OMB No. 0704-0188

The public reporting burden for this collection of information is estimated to average 1 hour per response, including the time for reviewing instructions, searching existing data sources, gathering and maintaining the data needed, and completing and reviewing the collection of information. Send comments regarding this burden estimate or any other aspect of this collection of information, including suggestions for reducing this burden, to Department of Defense, Washington Headquarters Services, Directorate for Information Operations and Reports (0704-0188), 1215 Jefferson Davis Highway, Suite 1204, Arlington, VA 22202-4302. Respondents should be aware that notwithstanding any other provision of law, no person shall be subject to any penalty for failing to comply with a collection of information if it does not display a currently valid OMB control number.
PLEASE DO NOT RETURN YOUR FORM TO THE ABOVE ADDRESS.

1. REPORT DATE *(DD-MM-YYYY)*	2. REPORT TYPE	3. DATES COVERED *(From - To)*
01-08-2009	Technical Memorandum	

4. TITLE AND SUBTITLE
Stability and Control Analysis of the F-15B Quiet Spike™ Aircraft

5a. CONTRACT NUMBER

5b. GRANT NUMBER

5c. PROGRAM ELEMENT NUMBER

6. AUTHOR(S)
Shaun C. McWherter, Cheng M. Moua, Joseph Gera, and Timothy H. Cox

5d. PROJECT NUMBER

5e. TASK NUMBER

5f. WORK UNIT NUMBER

7. PERFORMING ORGANIZATION NAME(S) AND ADDRESS(ES)
NASA Dryden Flight Research Center
P. O. Box 273
Edwards, California 93523-0273

8. PERFORMING ORGANIZATION REPORT NUMBER
H-2956

9. SPONSORING/MONITORING AGENCY NAME(S) AND ADDRESS(ES)
National Aeronautics and Space Administration
Washington, DC 20546-0001

10. SPONSORING/MONITOR'S ACRONYM(S)
NASA

11. SPONSORING/MONITORING REPORT NUMBER
NASA/TM-2009-214651

12. DISTRIBUTION/AVAILABILITY STATEMENT
Unclassified--Unlimited
Subject Category 08 Availability: NASA CASI (443) 757-5802 Distribution: Standard

13. SUPPLEMENTARY NOTES
McWherter, Moua, Cox, NASA Dryden Flight Research Center; Gera, AS&M, Inc.

14. ABSTRACT
The primary purpose of the Quiet Spike™ flight research program was to analyze the aerodynamic, structural, and mechanical proof-of-concept of a large multi-stage telescoping nose spike installed on the National Aeronautics and Space Administration Dryden Flight Research Center (Edwards, California) F-15B airplane. This report describes the preflight stability and control analysis performed to assess the effect of the spike on the stability, controllability, and handling qualities of the airplane; and to develop an envelope expansion approach to maintain safety of flight. The overall flight test objective was to collect flight data to validate the spike structural dynamics and loads model up to Mach 1.8. Other objectives included validating the mechanical feasibility of a morphing fuselage at operational conditions and determining the near-field shock wave characterization. The two main issues relevant to the stability and control objectives were the effects of the spike-influenced aerodynamics on the F-15B airplane flight dynamics, and the air data and angle-of-attack sensors. The analysis covered the sensitivity of the stability margins, and the handling qualities due to aerodynamic variation and the maneuvering limitations of the F-15B Quiet Spike™ configuration. The results of the analysis and the implications for the flight test program are also presented.

15. SUBJECT TERMS
Aerodynamic uncertainty, Envelope clearance, Handling qualities, Nose boom, Quiet Spike™, Simulation, Stability analysis

16. SECURITY CLASSIFICATION OF:			17. LIMITATION OF ABSTRACT	18. NUMBER OF PAGES	19b. NAME OF RESPONSIBLE PERSON
a. REPORT	b. ABSTRACT	c. THIS PAGE			STI Help Desk (email: help@sti.nasa.gov)
U	U	U	UU	53	19b. TELEPHONE NUMBER *(Include area code)* (443) 757-5802